Trabajo de Fin de Grado
Decoherence and entanglement in Quantum Physics

Alba Romero Rodríguez
Universidad de La Laguna (ULL)

Tutor: Santiago Brouard Martín
Universidad de La Laguna (ULL)

En San Cristóbal de La Laguna, a 04 de junio de 2017

Abstract

Most open systems are subjected to dissipative and/or decoherence processes. The latter is a process by which systems lose information that is transferred into the environment to which they are coupled, which can be appreciated in the time evolution of the non-diagonal elements of the density matrix that describes a quantum system (coherences), since they decay as time goes by. As for the dissipative processes, their effect can be seen in the time evolution of the diagonal elements of the density matrix (populations). That is why, in order to verify these effects in a series of open systems, their master equations will be determined. Afterwards, they will be solved, which will enable us to analyse and discuss the evolution of coherences and populations with time.

Contents

1 Introduction

Muchos sistemas abiertos se hallan sometidos a procesos disipativos y/o de decoherencia. Estos últimos procesos inducen pérdida de información que pasa al baño al que está acoplado el sistema, lo que queda plasmado en la evolución temporal de los elementos no diagonales de la matriz densidad que describe el sistema (coherencias), ya que decaen con el paso del tiempo. En lo referente a los procesos disipativos, su efecto queda patente en la evolución de los elementos diagonales de la matriz densidad (poblaciones). Es por ello que, con el fin de verificar estos procesos en una serie de sistemas abiertos, determinaremos sus respectivas ecuaciones maestras. A continuación se procederá a resolverlas, con lo que se podrá analizar y discutir la evolución temporal de las coherencias y poblaciones.

Quantum Mechanics is a very succesful field in Physics. Not only does it explain microscopic phenomena, but also macroscopic ones, just as recent studies have proved. For instance, a cryogenic version of the Weber bar -a gravity wave detector- must be treated as a quantum Harmonic Oscillator despite the fact that it weighs about a ton.

In Quantum mechanics, Physical systems are described by wavefunctions that evolve according to Schrödinger's equation. But it must be pointed out that this equation only applies for closed systems. This implies they go under a unitary evolution, i.e., the closed system will evolve as a pure state. Nevertheless, most Physical systems are open, i.e., they are coupled to the environment, which leads to a loss of coherence (or information) which is transfered to the latter. This is the so called **decoherence process**. Consequently, decoherence can be summarised as a non-unitary dynamics of the system due to its coupling to the environment. By coupling to the environment we mean either a measuring device that is performing measurements over the system, or some kind of external field in which the system is immersed. In either of those cases, both, the environment (i.e.:measuring device or external field) and the system, $\mathcal{S}$, itself must be treated Quantum mechanically and as a whole.

This also includes dissipative contributions, which are processes by which the populations of the quantum states (the density matrix of the system's diagonal elements) are modified by the interaction with the environment, and dephasing ones. Dephasing is a process of randomization of the relative phases of the quantum states. Both of these effects are caused by the entanglement of the system with the degrees of freedom of the environment, which leads to the non-unitary dynamics that have been mentioned above.

Now, decoherence will be explained mathematically. Let as assume we have a quantum detector that can be in either of these two states: $\{|d_a\rangle, |d_b\rangle\}$, performing measurements over a two level system that can be in either of these others: $\{|a\rangle, |b\rangle\}$. Given an initial state of the detector, let us say $|d_b\rangle$, if the system is in $|a\rangle$, then the detector will switch to $|d_a\rangle$, while it will remain unperturbed in the case the system is in $|b\rangle$:

$$|a\rangle |d_b\rangle \rightarrow |a\rangle |d_a\rangle \qquad |b\rangle |d_b\rangle \rightarrow |b\rangle |d_b\rangle . \tag{1}$$

Nevertheless, was the system to be in a superposition state: $|\psi_{initial}\rangle = \alpha |a\rangle + \beta |b\rangle$ then, we would get the so called correlated state after performing a measurement over it:

$$|\psi_c\rangle \equiv |\psi_{initial}\rangle |d_b\rangle \rightarrow \alpha |a\rangle |d_a\rangle + \beta |b\rangle |d_b\rangle , \tag{2}$$

where we have assumed the detector to be initially in $|d_b\rangle$. This state implies that if the detector measures $|d_a\rangle$, then the state of the system will be: $|a\rangle$. While was it to measure $|d_b\rangle$, then the state of the system would be: $|b\rangle$. However, this correlated state is unsatisfactory for describing a complete measurement. The reason is that, in reality, despite not knowing the outcome of a measurement, we do know the possible alternatives, and we can safely act as though only one of those has ocurred. The entire system can no longer be described

separately, i.e.: $H = H_{system} + H_{detector}$, where H, H_{system} and $H_{detector}$ are the Hamiltonians corresponding to the total system, the detector and the system $\mathcal{S}$, respectively.

As we are dealing with an open system, was the initial state of $\mathcal{S}$ to be a pure state, it would not evolve ramaining a pure state, but a mixed one. That is why the state of the system can no longer be described by a wavefunction but a density matrix. Consequently, that of the whole system will not only include the dynamics of the detector and the system separately, but also some mixed terms:

$$\begin{aligned}\rho^c = |\psi_c\rangle \langle\psi_c| = (\alpha |a\rangle |d_a\rangle + \beta |b\rangle |d_b\rangle)(\alpha^* \langle a| \langle d_a| + \beta^* \langle b| \langle d_b|) = \\ = |\alpha|^2 |a\rangle \langle a| |d_a\rangle \langle d_a| + |\beta|^2 |b\rangle \langle b| |d_b\rangle \langle d_b| + \alpha\beta^* |a\rangle \langle b| |d_a\rangle \langle d_b| + \alpha^*\beta |b\rangle \langle a| |d_b\rangle \langle d_a| .\end{aligned} \tag{3}$$

However, Von Neumann postulated that in addition to the unitary evolution above mentioned, there should be a non-unitary reduction of the state vector that would take the pure correlated state vector $|\psi_c\rangle$ into an appropriate mixture by getting rid off the off-diagonal elements, which express purely quantum correlations (entanglement). This way, we get the so called reduced density matrix:

$$\rho^r = |\psi_c\rangle \langle\psi_c| = (\alpha |a\rangle |d_a\rangle + \beta |b\rangle |d_b\rangle)(\alpha^* \langle a| \langle d_a| + \beta^* \langle b| \langle d_b|), \tag{4}$$

This one allows us to describe systems with the classical probabilities: $|\alpha|^2$ and $|\beta|^2$.

What's more, in the quantum case, ρ^c can be written differently according to the chosen basis. Let us take, as an example, the basis: $\Big\{ |c\rangle \equiv \frac{1}{\sqrt{2}}(|a\rangle + |b\rangle), |d\rangle \equiv \frac{1}{\sqrt{2}}(|a\rangle - |b\rangle) \Big\}$ and the values: $\alpha = -\beta = \frac{1}{\sqrt{2}}$. Consequently: $\Big\{ |a\rangle \equiv \frac{1}{\sqrt{2}}(|c\rangle + |d\rangle), |b\rangle \equiv \frac{1}{\sqrt{2}}(|c\rangle - |d\rangle) \Big\}$, and so $|\psi_c\rangle$ can be rewritten as:

$$\begin{aligned}|\psi_c\rangle \equiv |\psi_{initial}\rangle |d_b\rangle = \alpha |a\rangle |d_a\rangle + \beta |b\rangle |d_b\rangle = & \frac{1}{\sqrt{2}}\Big[\frac{1}{\sqrt{2}}(|c\rangle + |d\rangle) |d_a\rangle - \frac{1}{\sqrt{2}}(|c\rangle - |d\rangle) |d_b\rangle \Big] \\ \equiv & \frac{1}{\sqrt{2}}(|c\rangle |d_c\rangle - |d\rangle |d_d\rangle),\end{aligned} \tag{5}$$

where we have set: $|d_c\rangle = \frac{1}{\sqrt{2}}(|d_a\rangle + |d_b\rangle)$ and $|d_d\rangle = \frac{1}{\sqrt{2}}(|d_a\rangle - |d_b\rangle)$. With the result in Eq. (5), ρ^c can be written as:

$$\rho^c = |\psi_c\rangle \langle\psi_c| = \frac{1}{2}\Big[|c\rangle \langle c| |d_c\rangle \langle d_c| + |d\rangle \langle d| |d_d\rangle \langle d_d| + |c\rangle \langle d| |d_c\rangle \langle d_d| + |d\rangle \langle c| |d_d\rangle \langle d_c| \Big]. \tag{6}$$

If we just take the diagonal part:

$$(\rho^c)_{diag} = \frac{1}{2}\Big[|c\rangle \langle c| |d_c\rangle \langle d_c| + |d\rangle \langle d| |d_d\rangle \langle d_d| \Big], \tag{7}$$

it can be seen that it differs from the previous $(\rho^c)_{diag}$, which is obtained by substituting $\alpha = -\beta = \frac{1}{\sqrt{2}}$ and just taking the diagonal part of Eq.(3):

$$(\rho^c)_{diag} = \frac{1}{2}\Big[|a\rangle \langle a| |d_a\rangle \langle d_a| + |b\rangle \langle b| |d_b\rangle \langle d_b| \Big]. \tag{8}$$

As it can be noticed, the problem remains, since the quantum state of the system is still unknown. That is why we must proceed diffferently in order to get a measurement.

First and foremost, $|\psi_c\rangle$ must be obtained in the same way as it was shown above. Then, the total system (system plus detector) must be coupled to the environment (whose states will be labelled as $|\epsilon\rangle$) ir order to dispose of the information that had been lost into the latter. Mathematically speaking, that is:

$$|\psi_c\rangle |\epsilon_o\rangle \rightarrow \alpha |a\rangle |d_a\rangle |\epsilon_a\rangle + \beta |b\rangle |d_b\rangle |\epsilon_b\rangle \equiv |\psi\rangle . \tag{9}$$

If $\left\{|\epsilon_a\rangle, |\epsilon_b\rangle\right\}$ are orthogonal, a trace over the environment of Eq.(9) can be performed:

$$\rho_{TOTAL} = Tr_\epsilon |\psi\rangle \langle\psi| = \sum_i \langle\epsilon_i|\psi\rangle\langle\psi|\epsilon_i\rangle = \sum_i |\langle\epsilon_i|\psi\rangle|^2 = |\alpha|^2 |a\rangle \langle a| |d_a\rangle \langle d_a| + |\beta|^2 |b\rangle \langle b| |d_b\rangle \langle d_b|, \quad (10)$$

which coincides with ρ^r and where ρ_{TOTAL} is the density matrix for the whole system (system plus detector). Only unitary transformations have been performed, and no assumptions have been made in this latter procedure.[3].

Throughout this work, what the detector represented in this example will be named as the reservoir $\mathcal{R}$ (which plays the role of the environment) and then, the system will be $\mathcal{S}$.

In this project, two types of systems driven by thermal light will be considered. Nevertheless, we will begin by considering a general system interacting with the reservoir that will be particularised afterwards. First and foremost, the Master equation (describing the time eveolution of the density matrix) will be derived and then particularised for each of the systems according to [5] and [4] . On the one hand, we will be dealing with a cavity mode. On the other hand, a two level system subjected to a non-radiative dephasing will be studided. Afterwards, the solution for these differential equations will be calculated analitically and/or numerically. Finally, the effect of an external electric field over the cavity mode will also be studied. Some analitical and numerical calculus will be performed using Mathematica.

2 Master equation derivation for a small system $\mathcal{S}$ interacting with a reservoir $\mathcal{R}$ (thermal light)

En este apartado se derivará, de forma general, la ecuación maestra de un sistema cuántico en contacto con un entorno. Es decir, se justificará la evolución temporal de la matriz densidad que describe un sistema abierto en general. A continuación, partiendo de ese resultado, se particularizará la ecuación maestra para dos sistemas concretos, un "cavity mode driven by thermal light" y un sistema de dos niveles con un "non-radiative dephasing".

The following derivation has been taken from [5] and [4]. Let us consider a global system described by the Hamiltonian:

$$H = H_S + H_R + H_{RS}, \quad (11)$$

where H_R is the Hamiltonian associated to $\mathcal{R}$, H_S that to $\mathcal{S}$, and finally, H_{RS} represents the interaction between $\mathcal{S}$ and $\mathcal{R}$. The density operator of the total system is $\chi(t)$, and its time evolution is given by:

$$\dot{\chi(t)} = \frac{1}{i\hbar}[H, \chi(t)]. \quad (12)$$

Was H_{RS} to be sufficiently small, χ would evolve slowly in the interaction picture ($\tilde{\chi}$), so that is why we will be using the latter representation. Eq. (12) turns into:

$$\dot{\tilde{\chi}}(t) = \frac{1}{i\hbar}[\tilde{H}_{RS}(t), \tilde{\chi}(t)] \quad (13)$$

in the interaction picture, where $\tilde{\chi}(t) = e^{i(H_S+H_R)t/\hbar}\chi(t)e^{-i(H_S+H_R)t/\hbar}$ and $\tilde{H}_{RS}(t) = e^{i(H_S+H_R)t/\hbar}H_{RS}e^{-i(H_S+H_R)t/\hbar}$. Eq.(13) can be integrated from 0 to t and then susbtitute the result within Eq.(12), so that we get:

$$\tilde{\chi}(t) = \frac{1}{i\hbar}[\tilde{H}_{RS}(t), \tilde{\chi}(0)] - \frac{1}{\hbar^2}\int_0^t dt'[\tilde{H}_{RS}(t), [\tilde{H}_{RS}(t'), \tilde{\chi}(t')]]. \quad (14)$$

Since we are only interested in the evolution of system $\mathcal{S}$, we will perform the trace over $\mathcal{R}$ of $\tilde{\chi}(t)$, so that we end up with a reduced density operator $\rho(t) = Tr_R[\chi(t)]$ that describes $\mathcal{S}$. Let us now consider that the interaction between $\mathcal{R}$ and $\mathcal{S}$ is turned on at $t = 0$ and that there does not exist correlations between them at that time. Consequently, the density matrix can be factorized as a product of two operators, each belonging to one of the systems: $\chi(0) = \rho(0)R_0 = \tilde{\chi}(0)$. From now onwards, we will be dealing with $\rho(t)$. That is why we now proceed onto tracing over $\mathcal{R}$ Eq.(14), which leads to:

$$\dot{\tilde{\rho}}(t) = \frac{1}{i\hbar} Tr_R[\tilde{H}_{RS}(t), \tilde{\chi}(0)] - \frac{1}{\hbar^2} \int_0^t dt' Tr_R[\tilde{H}_{RS}(t), [\tilde{H}_{RS}(t'), \tilde{\chi}(t')]]. \tag{15}$$

It has been denoted: $Tr_R(\tilde{\chi}(t)) = e^{iH_s t/\hbar} \rho e^{-iH_s t/\hbar} = \tilde{\rho}(t)$.

Up to this point, no approximations have been considered. Nevertheless, it must be noted that $\mathcal{R}$ can be considered as being unperturbed so that $\tilde{R}(t) \simeq \tilde{R}(0) \equiv R_0$ (which has already been used), where $\tilde{R}(t) = Tr_S \tilde{\chi}(t)$.

Furthermore, $\mathcal{R}$ can be assumed to be in a stationary state, and consequently: $[R_0, H_R] = 0 \Rightarrow R_0 = \sum_\mu p_\mu |\mu\rangle \langle\mu|$, where $|\mu\rangle$ are the eigenstates of H_R and p_μ the probabilities associated to each of these states.

What's more, it can also be assumed that the interaction between the two systems is given by the product of two operators belonging to each of them: $H_{SR} = -SR$ which, in the interaction picture is: $\tilde{H_{SR}}(t) = -\tilde{S}(t)\tilde{R}(t)$. If it is asssumed that $Tr_R[RR_0] = Tr_R[\tilde{R}R_0] = 0$ then, $Tr_R[\tilde{H}_{SR}(t)R_0] = -\tilde{S}Tr_R[\tilde{R}R_0] = 0$. This can be guaranteed if it is assumed that the $\mathcal{R}$'s operators coupling to $\mathcal{S}$ have zero mean in the state R_0. Was this condition not to be satisfied, the total Hamiltonian could be redifined so that the new interaction Hamiltonian verified this condition:

$$\begin{gathered} H = H_S + H_R + H_{SR} \rightarrow H = H_S + H_R + H_{SR} + \hat{O_S} \otimes \mathbb{I}_\mathbb{R} - \hat{O_S} \otimes \mathbb{I}_\mathbb{R} \\ H_S{}' \equiv H_S + \hat{O_S} \otimes \mathbb{I}_\mathbb{R} \quad \wedge \quad H_{SR}{}' \equiv H_{SR} - \hat{O_S} \otimes \mathbb{I}_\mathbb{R} / Tr_R[H_{SR}{}'(t)R_0] = 0, \end{gathered} \tag{16}$$

where $\hat{O_S}$ is a certain operator $\in \mathcal{S}$.

In fact, this is the case of one of the systems that it will be dealt with in this work, the two state atom in thermal equilibrium with non-radiative dephasing.

With this result, Eq.(15) can be simplified:

$$\dot{\tilde{\rho}}(t) = -\frac{1}{\hbar^2} \int_0^t dt' Tr_R[\tilde{H}_{RS}(t), [\tilde{H}_{RS}(t'), \tilde{\chi}(t')]]. \tag{17}$$

But it must be kept in mind that for $t > 0$, correlations may arise between $\mathcal{R}$ and $\mathcal{S}$. For this reason, a term that accounts for them must be added: $\tilde{\chi}(t) = \tilde{\rho}(t)R_0 + O(H_{SR})$.

Let us now consider that higher than second order terms (higher than $\tilde{H}_{SR}(t)^2$) can be neglected (this is known as Born approximation). For this reason, Eq. (17) can be further simplified:

$$\dot{\tilde{\rho}}(t) = -\frac{1}{\hbar^2} \int_0^t dt' Tr_R[\tilde{H}_{RS}(t), [\tilde{H}_{RS}(t'), \tilde{\rho}(t')R_0]]. \tag{18}$$

The behaviour of the whole system will be considered to be Markoffian (its future behaviour does not depend on the past but just on the present state of the system), since the reservoir $\mathcal{R}$ is large enough (and in thermal equilibrium) so as not to keep changes induced by $\mathcal{S}$ over it for a long time, which will be reverted reciprocally into $\mathcal{S}$. That is, $\mathcal{S}$ will not be affected by past events, given that, for any change in it, it will rapidly go

into $\mathcal{R}$, which will quickly return to the previous state. For that reason, $\tilde{\rho}(t')$ will turn into $\tilde{\rho}(t)$ in Eq. (18), leading to:

$$\dot{\tilde{\rho}}(t) = -\frac{1}{\hbar^2}\int_0^t dt' Tr_R[\tilde{H}_{RS}(t), [\tilde{H}_{RS}(t'), \tilde{\rho}(t)R_0]]. \tag{19}$$

Later on in this section, the exact reason that allows us to assume that our system is undergoing a Markoffian process will be exposed.

Now, let us make the model slightly more general by setting that the interaction between the two systems is given by the sum of the product of operators belonging to each system, s_i from $\mathcal{S}$ and Γ_i from $\mathcal{R}$: $H_{SR} = \hbar\sum_i s_i\Gamma_i$ which, in the interaction picture is $\mathcal{R}$: $\tilde{H}_{SR} = \hbar\sum_i \tilde{s}_i\tilde{\Gamma}_i$. So going back to the Eq.(18) and substituting this expression we get:

$$\dot{\tilde{\rho}}(t) = -\sum_i\sum_j\int_0^t dt' Tr_R[\tilde{s}_i(t)\tilde{\Gamma}_i(t), [\tilde{s}_j(t')\tilde{\Gamma}_j(t'), \tilde{\rho}(t)R_0]]. \tag{20}$$

Now, by using a cyclic property of the trace for any three given operators A,B and C: $Tr(ABC) = Tr(CAB) = Tr(BCA)$, Eq. (20) can be rewritten such as:

$$\begin{aligned}\dot{\tilde{\rho}}(t) = -\sum_i\sum_j\int_0^t dt' Tr_R[&\tilde{s}_i(t)\tilde{\Gamma}_i(t)\tilde{s}_j(t')\tilde{\Gamma}_j(t')\tilde{\rho}(t')R_0 - \tilde{s}_j(t')\tilde{\Gamma}_j(t')\tilde{\rho}(t')R_0\tilde{s}_i(t)\tilde{\Gamma}_i(t)\\ &-\tilde{s}_i(t)\tilde{\Gamma}_i(t)\tilde{\rho}(t')R_0\tilde{s}_j(t')\tilde{\Gamma}_j(t') + \tilde{\rho}(t')R_0\tilde{s}_j(t')\tilde{\Gamma}_j(t')\tilde{s}_i(t)\tilde{\Gamma}_i(t)] =\\ = -\sum_i\sum_j\int_0^t dt'\Big\{&[\tilde{s}_i(t)\tilde{s}_j(t')\tilde{\rho}(t') - \tilde{s}_j(t')\tilde{\rho}(t')\tilde{s}_i(t)]Tr_R[R_0\tilde{\Gamma}_i(t)\tilde{\Gamma}_j(t')]\\ &-[\tilde{s}_i(t)\tilde{\rho}(t')\tilde{s}_j(t') - \tilde{\rho}(t')\tilde{s}_j(t')\tilde{s}_i(t)]Tr_R[R_0\tilde{\Gamma}_j(t')\tilde{\Gamma}_i(t)]\Big\}.\end{aligned} \tag{21}$$

Finally, it is known that the trace over $\mathcal{R}$ of operators belonging to it and which are multiplied by the density operator of $\mathcal{R}$ (R_0) is the average value of these operators. For this reason: $Tr_R[R_0\tilde{\Gamma}_i(t)\tilde{\Gamma}_j(t')] = \langle\tilde{\Gamma}_i(t)\tilde{\Gamma}_j(t')\rangle_R$ and $Tr_R[R_0\tilde{\Gamma}_j(t')\tilde{\Gamma}_i(t)] = \langle\tilde{\Gamma}_j(t')\tilde{\Gamma}_i(t)\rangle_R$. If these correlation functions decay rapidly on the time scale on which $\tilde{\rho}(t)$ varies, then the so called Markoffian process ($\tilde{\rho}(t') \to \tilde{\rho}(t)$) is justified.

This implies that in the problem that we are dealing with there are two different time scales. On the one hand, a slow time scale, in which $\mathcal{S}$ varies, and a fast one caracterizing the evolution of $\mathcal{R}$.

2.1 Cavity mode

In this case, our Hamiltonian is the sum of the following three Hamiltonians:

$$H_S = \hbar\omega_c a^\dagger a, \tag{22}$$

$$H_R = \sum_j \hbar\omega_j {r_j}^\dagger r_j \tag{23}$$

and

$$H_{SR} = \sum_j \hbar({\kappa_j}^* a {r_j}^\dagger + \kappa_j a^\dagger r_j) = \hbar(a\Gamma^\dagger + a^+\Gamma), \tag{24}$$

where a and $a^\dagger$ are the anhiilation and creation operators, respectively, of the system $\mathcal{S}$, which is a harmonic oscillator with frequency ω_c; r_j and ${r_j}^\dagger$ are those corresponding to the reservoir $\mathcal{R}$ (which is a collection

of harmonic oscillators, each having frequency ω_j). Finally, the oscillator of $\mathcal{S}$ couples to each of those in $\mathcal{R}$ by a coupling constant κ_j in the Rotating Wave Approximation (RWA)[7]. The reason why this approximation can be used is that the problem we are dealing with is non-integrable. For this reason, in order to obtain an analitical approximate solution, the RWA is used. It basically approximates $2\cos\theta$ by $e^{i\theta}$, since $2\cos\theta = e^{i\theta} + e^{-i\theta} = e^{i\theta}(1 + e^{-2i\theta})$ and, given that $e^{-2i\theta}$ goes away quicker than $e^{i\theta}$, then it can be neglected. For this reason, since the thermal light in the cavity goes clasically as a trigonometric function, this approximation is applied.

Let us assume that $\mathcal{R}$ is in thermal equilibrium (at temperature T). In this case, and if we relate to the master equation derivation above detailed, R_0 is given by: $R_0 = \prod_j e^{\frac{-\hbar\omega_j {r_j}^\dagger r_j}{\kappa_B T}}\left(1 - e^{\frac{-\hbar\omega_j}{\kappa_B T}}\right)$, which represents thermal light. In it, κ_B can be seen, which is Boltzmann's constant.

In the present case, since $\mathcal{S}$ is a harmonic oscillator, the s_i operators used in the first section can be identified with the annhiilation and creation operators present in H_S: $s_1 = a$ and $s_2 = a^\dagger$. By looking at H_{SR} (see Eq. (24)), it can be noticed that we have used $\sum_j \kappa_j {r_j}^\dagger = \Gamma^\dagger$ and $\sum_j \kappa_j r_j = \Gamma$ which will be renamed such as: $\Gamma^\dagger \equiv \Gamma_1$ and $\Gamma \equiv \Gamma_2$.

In the interaction picture, the operators are:

$$\begin{aligned}
&\tilde{s}_1(t) = e^{i\omega_c a^\dagger a t} a e^{-i\omega_c a^\dagger a t} = a e^{-i\omega_c t}; \qquad \tilde{s}_2(t) = e^{i\omega_c a^\dagger a t} a^\dagger e^{-i\omega_c a^\dagger a t} = a^\dagger e^{i\omega_c t} \\
&\tilde{\Gamma}_1(t) = e^{i\sum_n \omega_n r_n^\dagger r_n t} \sum_j {\kappa_j}^* {r_j}^\dagger e^{-i\sum_m \omega_m r_m^\dagger r_m t} = \sum_j {\kappa_j}^* {r_j}^\dagger e^{i\omega_j t}; \qquad \tilde{\Gamma}_2(t) = \sum_j \kappa_j r_j e^{-i\omega_j t},
\end{aligned} \tag{25}$$

where the second equality is obtained after a series of calculations. As an example, the calculus corresponding to $\tilde{s}_1(t)$ is performed:

$$\begin{aligned}
\tilde{s}_1(t) &= e^{i\omega_c N t} a e^{-i\omega_c N t} \\
e^{i\omega_c n t} &= \mathbb{I} + i\omega_c N t - \frac{1}{2}(\omega_c N t)^2 + ... \Rightarrow e^{-i\omega_c n t} = \mathbb{I} - i\omega_c N t - \frac{1}{2}(\omega_c N t)^2 + ... \\
\tilde{s}_1(t) &= [\mathbb{I} + i\omega_c N t - \frac{1}{2}(\omega_c N t)^2 + ...] a [\mathbb{I} - i\omega_c N t - \frac{1}{2}(\omega_c N t)^2 + ...] \\
&= a - i\omega_c a N t - \frac{1}{2} a (\omega_c N t)^2 + i\omega_c N a t + {\omega_c}^2 N a N t^2 - \frac{1}{2}(\omega_c N t)^2 a + ... \\
&= a + i\omega_c t [N, a] - \frac{1}{2}(\omega_c t)^2 [a N^2 + N^2 a - 2 N a N] + ... \\
[N, a] &= -a \Rightarrow \quad a N^2 = N a N + a N \quad \wedge \quad N^2 a = -N a + N a N \Rightarrow \\
\tilde{s}_1(t) &= a - i\omega_c t a - \frac{1}{2}(\omega_c t)^2 [a, N] + ... = a[\mathbb{I} - i\omega_c t + \frac{1}{2}(\omega_c t)^2 + ...] = a e^{-i\omega_c t},
\end{aligned} \tag{26}$$

where $a^\dagger a \equiv N$ has been set, i.e., the Number operator.

Now, going back to Eq.(21) and substituting all the operators by the ones just mentioned, an integral with sixteen terms will be obtained, given that $i, j = 1, 2$ in the present case. As for the reservoir correlation

functions, the ones that reqcuire to be calculated can be seen:

$$\begin{aligned}
\langle\tilde{\Gamma}^{\dagger}(t)\tilde{\Gamma}(t')\rangle_R &= \sum_j |\kappa_j|^2 e^{i\omega_j(t-t')}\langle r_j^{\dagger}r_j\rangle_R = \sum_j |\kappa_j|^2 e^{i\omega_j(t-t')}\bar{n}(\omega_j,T)\\
\langle\tilde{\Gamma}(t)\tilde{\Gamma}^{\dagger}(t')\rangle_R &= \sum_j |\kappa_j|^2 e^{-i\omega_j(t-t')}\langle r_j r_j^{\dagger}\rangle_R = \sum_j |\kappa_j|^2 e^{-i\omega_j(t-t')}[1+\bar{n}(\omega_j,T)]\\
\langle\tilde{\Gamma}^{\dagger}(t)\tilde{\Gamma}^{\dagger}(t')\rangle_R &= \sum_j (\kappa_j^*)^2 e^{i\omega_j(t+t')}\langle r_j^{\dagger}r_j^{\dagger}\rangle_R = 0\\
\langle\tilde{\Gamma}(t)\tilde{\Gamma}(t')\rangle_R &= \sum_j (\kappa_j)^2 e^{-i\omega_j(t+t')}\langle r_j r_j\rangle_R = 0,
\end{aligned} \tag{27}$$

for which the expressions in Eq.(25) have been used. It has also been introduced within Eq.(27) the fact that $\langle r_j^{\dagger}r_j\rangle_R = \langle n_j\rangle_R = \bar{n}(\omega_j,T)$, where n_j is the number operator for the j-th oscillator, that is, we get the average number of photons in the j-th mode, which is given by:

$$\bar{n}(\omega_j,T) = \frac{e^{-\frac{\hbar\omega_j}{\kappa_j T}}}{1-e^{-\frac{\hbar\omega_j}{\kappa_j T}}}. \tag{28}$$

It is also known that $[r_j, r_j^{\dagger}] = 1 \Rightarrow r_j r_j^{\dagger} = 1 + r_j^{\dagger}r_j \Rightarrow \langle r_j r_j^{\dagger}\rangle_R = 1 + \bar{n}(\omega_j,T)$. In addition to this, it is known that $\langle r_j^{\dagger}r_j^{\dagger}\rangle_R = 0$ and $\langle r_j r_j\rangle_R = 0$.

With the results in Eq.(27) and making a change of variables: $\tau = t - t' \Rightarrow t' = t - \tau$, the equation above mentioned which contained sixteen terms will be reduced to one with eight:

$$\begin{aligned}
\dot{\tilde{\rho}} = -\int_0^t d\tau \Big\{ &[aa^{\dagger}\tilde{\rho}(t-\tau) - a^{\dagger}\tilde{\rho}(t-\tau)a]e^{-i\omega_c\tau}\langle\tilde{\Gamma}^{\dagger}(t)\tilde{\Gamma}(t-\tau)\rangle_R + h.c.\\
&[a^{\dagger}a\tilde{\rho}(t-\tau) - a\tilde{\rho}(t-\tau)a^{\dagger}]e^{i\omega_c\tau}\langle\tilde{\Gamma}(t)\tilde{\Gamma}^{\dagger}(t-\tau)\rangle_R + h.c\Big\}.
\end{aligned} \tag{29}$$

At this point, rather than having a quantized number of frequencies in $\mathcal{R}$, let us assume that the frequency is a continuous value. Then, we will introduce the density of states:$g(\omega)$ so that $g(\omega)d\omega$ gives the number of oscillators with frequency $\in [\omega, \omega + d\omega]$. Furthermore, the change of variables above mentioned will be performed:$\tau = t - t' \Rightarrow t' = t - \tau$. Consequently, the non-null averages in Eq.(27) can be rewritten as:

$$\langle\tilde{\Gamma}^{\dagger}(t)\tilde{\Gamma}(t-\tau)\rangle_R = \int_0^{\infty} d\omega g(\omega)|\kappa(\omega)|^2 e^{i\omega\tau}\bar{n}(\omega,T); \qquad \langle\tilde{\Gamma}(t)\tilde{\Gamma}^{\dagger}(t-\tau)\rangle_R = \int_0^{\infty} d\omega g(\omega)|\kappa(\omega)|^2 e^{-i\omega\tau}[1+\bar{n}(\omega,T)]. \tag{30}$$

It can be proved (see [5]) that the reservoir correlation time (τ) is much smaller than the time scale in which $\tilde{\rho}$ suffers changes. Consequently, $\tilde{\rho}(t-\tau)$ can be approximated by $\tilde{\rho}(t)$. This way, Eq.(29) turns into:

$$\dot{\tilde{\rho}} = \alpha(a\tilde{\rho}a^{\dagger} - a^{\dagger}a\tilde{\rho}) + \beta(a\tilde{\rho}a^{\dagger} + a^{\dagger}a\tilde{\rho} - a^{\dagger}a\tilde{\rho} - \tilde{\rho}aa^{\dagger}) + h.c., \tag{31}$$

where α and β are given by:

$$\alpha = \int_0^t d\tau \int_0^{\infty} d\omega e^{-i(\omega-\omega_c)\tau} g(\omega)|\kappa(\omega)|^2; \qquad \beta = \int_0^t d\tau \int_0^{\infty} d\omega e^{-i(\omega-\omega_c)\tau} g(\omega)|\kappa(\omega)|^2 \bar{n}(\omega,T). \tag{32}$$

Since $\tau << t$, the time integrals in Eq. (32) can be approximated using the following result:

$$\lim_{t\to\infty}\int_0^t d\tau e^{-i(\omega-\omega_c)\tau} = \pi\delta(\omega-\omega_c) + i\frac{P}{\omega_c-\omega}, \tag{33}$$

where P is the Cauchy princial value. That way, α and β turn into:

$$\alpha = \pi g(\omega_c)|\kappa(\omega_c)|^2 + i\Delta; \qquad \beta = \pi g(\omega_c)|\kappa(\omega_c)|^2\bar{n}(\omega_c) + i\Delta', \tag{34}$$

where $\Delta = P\int_0^\infty d\omega \frac{g(\omega)|\kappa(\omega)|^2}{\omega_c - \omega}$ and $\Delta' = P\int_0^\infty d\omega \frac{g(\omega)|\kappa(\omega)|^2}{\omega_c - \omega}\bar{n}(\omega)$.

Finally, by setting: $\kappa \equiv \pi g(\omega_c)|\kappa(\omega_c)|^2$, $\bar{n} \equiv \bar{n}(\omega_c)$, $\omega_{c'} \equiv \omega_c + \Delta$ and transforming $\dot{\hat{\rho}}$ back into the Scrhödinger representation, the master equation for the cavity mode driven by thermal light is obtained:

$$\dot{\rho} = -i\omega_{c'}[a^\dagger a, \rho] + \kappa(2a\rho a^\dagger - a^\dagger a\rho - \rho a^\dagger a) + 2\kappa\bar{n}(a\rho a^\dagger + a^+\rho a - a^\dagger a\rho - \rho a a^\dagger).[4][5] \tag{35}$$

In the following equations:

$$\dot{\rho_{nn}} = 2\kappa[(n+1)\rho_{(n+1)(n+1)}(1+\bar{n}) + \bar{n}n\rho_{(n-1)(n-1)} - (n + 2\bar{n}n + \bar{n})\rho_{nn}], \tag{36}$$

and

$$\dot{\rho_{nm}} = -\rho_{nm}[i\omega_{c'}(n-m) + \kappa(n+m) + 2\kappa\bar{n}(n+m+1)] + \rho_{(n+1)(m+1)}2\kappa\sqrt{(m+1)(n+1)}(1+\bar{n}) + \sqrt{nm}2\kappa\bar{n}\rho_{(n-1)(m-1)} \tag{37}$$

the master equations for the populations and the coherences, respectively, have been calculated.

2.1.1 Interpretation of the master equation for the populations

In order to interpret Eq.(36), let us now change the notation slightly, just as follows: $\rho_{nn} \equiv P_n$, which enables us to rewritte it as:

$$\dot{P_n} = 2\kappa[(n+1)(1+\bar{n})P_{n+1} + \bar{n}nP_{(n-1)} - \bar{n}(n+1)P_n - n(\bar{n}+1)P_n]. \tag{38}$$

Four terms have been written down, among which two are related to the $|n\rangle$ level probability. Each of the factors accompanying the probabilities has been separated such as a differentiated processes in Figure 1. If we have a look at it, it represents a subspace of the harmonic oscillator: $\{|n-1\rangle, |n\rangle, |n+1\rangle\}$.

We have tried to give an explanation to these processes as follows:

(1) The $|n\rangle$ level increases its population due to the fact that there is a flux of population from $|n+1\rangle$ to $|n\rangle$ with a rate: $2\kappa(1+\bar{n})(1+n)$.

(2) The $|n\rangle$ level increases its population thanks to $|n-1\rangle$ level, being the rate: $2\kappa\bar{n}n$.

(3) The $|n\rangle$ level loses population which is gained by $|n+1\rangle$ level with a rate: $2\kappa\bar{n}(n+1)$.

(4) The $|n-1\rangle$ level gains population coming from the $|n\rangle$ level with a rate: $2\kappa\bar{n}n$.

Nevertheless, it still is not clear enough whether this explanation is fully correct. For this reason, let us now considerer the rates of change associated to the levels right above and below the one considered ($|n\rangle$), which can be seen in:

$$\dot{P_{n+1}} = 2\kappa[(n+2)(1+\bar{n})P_{n+2} + \bar{n}(n+1)P_{(n+1)} - \bar{n}(n+2)P_{n+1} - (n+1)(\bar{n}+1)P_{n+1}], \tag{39}$$

and

$$\dot{P_{n-1}} = 2\kappa[n(1+\bar{n})P_n + \bar{n}(n-1)P_{(n-2)} - \bar{n}nP_{n-1} - (n-1)(\bar{n}+1)P_{n-1}], \tag{40}$$

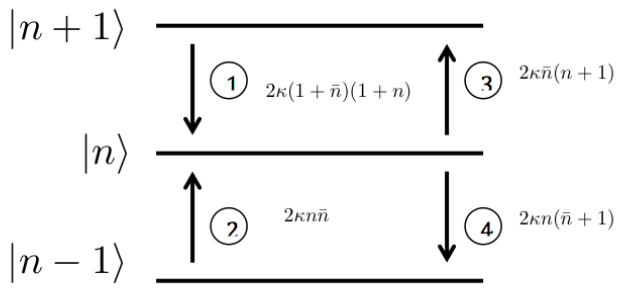

Figure 1: Cavity mode driven by thermal light for the subspace:$\{|n-1\rangle, |n\rangle, |n+1\rangle\}$

respectively. By following the same procedure as for the n^{th} level, we now chose another two subspaces: $\{|n\rangle, |n+1\rangle, |n+2\rangle\}$ and $\{|n-2\rangle, |n-1\rangle, |n\rangle\}$, which are plotted in Figures 2 and 3, respectively. Again, the factors in Eq.(39) and Eq.(40) have been associated with certain processes. If we have a look at them, it can be noticed that process (6) is exactly (3) and (8) is identical to (1). Furthermore, (9) is (4) and (11) is (2). For these reasons, it can be concluded that the explanation given for the processes (1), (2), (3) and (4) is correct.

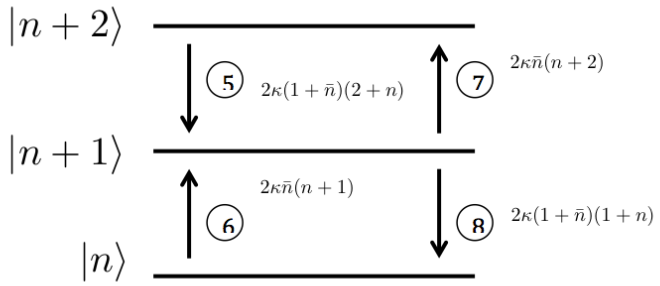

Figure 2: Cavity mode driven by thermal light for the subspace:$\{|n+2\rangle, |n+1\rangle, |n\rangle\}$

2.2 Two level system

Let us assume a two level system with levels $|1\rangle$ with energy E_1 and $|2\rangle$ with E_2. Then, the unperturbed Hamiltonian is $H_S = E_1 |1\rangle\langle 1| + E_1 |1\rangle\langle 1|$. Now, by using Pauli matrices, H_S can be rewritten as follows: $H_S = \frac{1}{2}(E_1+E_2)\mathbb{I}+\frac{1}{2}(E_1-E_2)\sigma_z$. The first term can be neglected if the lowest value of energy (0) in the middle

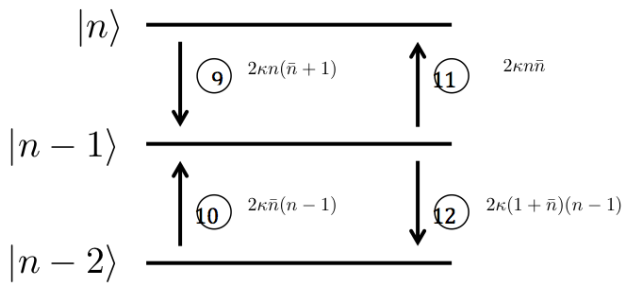

Figure 3: Cavity mode driven by thermal light for the subspace:$\{|n\rangle, |n-1\rangle, |n-2\rangle\}$

of the atomic transition is set. What's more, by renaming $E_1 - E_2 = \omega_A\hbar$, we end up having:$H_S = \frac{1}{2}\hbar\omega_A\sigma_z$.

Since this two level system is coupled to an electromagnetic field, the Hamiltonian of the latter must also be considered:

$$H_R = \sum_{\vec{k}\lambda} \hbar\omega_\kappa {r_{\vec{k}\lambda}}^\dagger r_{\vec{k}\lambda}, \tag{41}$$

as well as a Hamiltonian that accounts for the interaction between both systems:

$$H_{SR} = \sum_{\vec{k}\lambda} \hbar(\kappa_{\vec{k}\lambda}{}^* {r_{\vec{k}\lambda}}^\dagger \sigma_- + \kappa_{\vec{k}\lambda} r_{\vec{k}\lambda}\sigma_+). \tag{42}$$

It can be seen that new operators have been introduced. That is the case of the pseudo-spin Pauli matrices:

$$\sigma_- = \begin{bmatrix} 0 & 0 \\ 1 & 0 \end{bmatrix}, \qquad \sigma_+ = \begin{bmatrix} 0 & 1 \\ 0 & 0 \end{bmatrix}, \qquad \sigma_z = \begin{bmatrix} 1 & 0 \\ 0 & -1 \end{bmatrix}., \tag{43}$$

which comply the relations:

$$\sigma_\pm = \frac{1}{2}(\sigma_x \pm i\sigma_y),, \tag{44}$$

as well as the commutation relations:

$$[\sigma_+, \sigma_-] = \sigma_z \qquad [\sigma_\pm, \sigma_z] = \mp 2\sigma_\pm. \tag{45}$$

By looking at them, it can be noticed that σ_- acts lowering the energy of the system, while σ_+ increases it. That is why they are commonly called atomic lowering and raising operators, respectively.

Let us proceed with the description of the Hamiltonians in Eq.(41) and Eq.(42). In both of them, there is a summation over all the harmonic oscillators of which the reservoir (the EM field) is composed. Each of them has a wavevector: $\vec{k}$ and a certain polarization: λ, as well as a frequency: $\omega_{\vec{k}}$. There are a couple of constants:

$$\kappa_{\vec{k},\lambda} = -ie^{i\vec{k}\vec{r}_A}\sqrt{\frac{\omega_{\vec{k}}}{2\hbar\epsilon_o V}}\hat{e}_{\vec{k},\lambda}\vec{\mu}_{12} \tag{46}$$

in which $\hat{e}_{\vec{k},\lambda}$ is the unit polarization vector and $\vec{\mu}_{12}$ is the element between the states $|1\rangle$ and $|2\rangle$ of the dipole moment ($\vec{\mu} = e\hat{q}$, for e being the electron charge and $\hat{q}$ the coordinate operator for the bound electron). In

addition to this, it must be mentioned that the two level system is placed at $\vec{r}_A$ and V is the quantization volume.

Now, let us resort to Eq.(21), in which the operators $\tilde{s}_i$ and $\tilde{\Gamma}_i$ will be substituted by those corresponding to this particular system. For that purpose, we must begin by comparing Eq.(42) to $H_{SR} = \hbar \sum_i s_i \Gamma_i$ (which was used in the previous section). We can identify the relations seen below:

$$s_1 = \sigma_-, \quad s_2 = \sigma_+, \quad \Gamma_1 \equiv \Gamma^\dagger = \sum_{\vec{k}\lambda} {\kappa_{\vec{k}\lambda}}^* {r_{\vec{k}\lambda}}^\dagger \sigma_-, \quad \Gamma_2 \equiv \Gamma = \sum_{\vec{k}\lambda} \kappa_{\vec{k}\lambda} r_{\vec{k}\lambda} \sigma_+. \tag{47}$$

These relations turn into those seen below (in the interaction picture):

$$\begin{aligned}
\tilde{s}_1(t) =& e^{\frac{i\omega_A \sigma_z t}{2}} \sigma_- e^{\frac{-i\omega_A \sigma_z t}{2}} = \sigma_- e^{-i\omega_A t}; \qquad \tilde{s}_2(t) = e^{\frac{i\omega_A \sigma_z t}{2}} \sigma_+ e^{\frac{-i\omega_A \sigma_z t}{2}} = \sigma_+ e^{i\omega_A t} \\
\tilde{\Gamma}_1(t) \equiv \tilde{\Gamma}^\dagger(t) =& e^{it \sum_{\vec{k}\lambda} \omega_\kappa {r_{\vec{k}\lambda}}^\dagger r_{\vec{k}\lambda}} \sum_{\vec{k}\lambda} {\kappa_{\vec{k}\lambda}}^* {r_{\vec{k}\lambda}}^\dagger \sigma_- e^{-it \sum_{\vec{k}\lambda} \omega_\kappa {r_{\vec{k}\lambda}}^\dagger r_{\vec{k}\lambda}} = \sum_{\vec{k}\lambda} {\kappa_{\vec{k}\lambda}}^* {r_{\vec{k}\lambda}}^\dagger \sigma_- e^{-i\omega_{\vec{k}} t} \\
\tilde{\Gamma}_2(t) \equiv \tilde{\Gamma}(t) =& e^{it \sum_{\vec{k}\lambda} \omega_\kappa {r_{\vec{k}\lambda}}^\dagger r_{\vec{k}\lambda}} \sum_{\vec{k}\lambda} {\kappa_{\vec{k}\lambda}}^* {r_{\vec{k}\lambda}}^\dagger \sigma_+ e^{-it \sum_{\vec{k}\lambda} \omega_\kappa {r_{\vec{k}\lambda}}^\dagger r_{\vec{k}\lambda}} = \sum_{\vec{k}\lambda} \kappa_{\vec{k}\lambda} r_{\vec{k}\lambda} \sigma_+ e^{-i\omega_{\vec{k}} t}.
\end{aligned} \tag{48}$$

If we look closely at relations in Eq.(25), a big resemblance between them and those in Eq.(48) can be clearly seen. That is why the very same procedure done for the cavity mode has been followed to obtain the two level system master equation. Nevertheless, there are two details that need to be pointed out. First of all, while in the case of the cavity mode there was a summation over the reservoir harmonic oscillators, in this case, the summation is over wavevector directions and polarization states. Secondly, different commutation relations have been used.

Keeping these points in mind, all that is left is replacing a by σ_-, $a^\dagger$ by σ_+ and ω_c by ω_A in Eq.(31). Furthermore, if we keep in mind relations in Eq.(34) and define:

$$\gamma = 2\pi \sum_\lambda \int d^3k g(\vec{k}) |\kappa(\vec{k}, \lambda)|^2 \delta(kc - \omega_A) = 2\pi \sum_\lambda g(\omega_A) |\kappa(\omega_A, \lambda)|^2 \to 2\kappa, \tag{49}$$

it is clear that α and β from Eq.(31) are:$\alpha = \kappa + i\Delta$ and $\beta = \kappa\bar{n} + i\Delta'$. Consequently, by rearranging terms in Eq.(31) we get:

$$\dot{\tilde{\rho}} = \Big[\frac{\gamma}{2}(\bar{n}+1) + i(\Delta' + \Delta)\Big](\sigma_- \tilde{\rho} \sigma_+ - \sigma_+ \sigma_- \tilde{\rho}) + h.c. + \Big(\frac{\gamma}{2}\bar{n} + i\Delta'\Big)(\sigma_- \tilde{\rho}\sigma_+ + \sigma_+ \tilde{\rho}\sigma_- - \sigma_+\sigma_-\tilde{\rho} - \tilde{\rho}\sigma_-\sigma_+) + h.c., \tag{50}$$

where $\bar{n} = \bar{n}(\omega_A, T)$, $\Delta = \sum_\lambda P \int d^3k \frac{g(\vec{k}) |\kappa(\vec{k},\lambda)|^2}{\omega_A - kc}$ and $\Delta' = \sum_\lambda P \int d^3k \frac{g(\vec{k}) |\kappa(\vec{k},\lambda)|^2}{\omega_A - kc} \bar{n}(kc, T)$.

If we now proceed onto developing the hermitic conjugate terms in Eq. (50) we get:

$$\begin{aligned}
\dot{\tilde{\rho}} =& \frac{\gamma}{2}(\bar{n}+1)(2\sigma_-\tilde{\rho}\sigma_+ - \sigma_+\sigma_-\tilde{\rho} - \tilde{\rho}\sigma_+\sigma_-) - i(\Delta + \Delta')[\sigma_+\sigma_-, \tilde{\rho}] + \\
&+ \frac{\gamma}{2}\bar{n}(2\sigma_+\tilde{\rho}\sigma_- - \sigma_-\sigma_+\tilde{\rho} - \tilde{\rho}\sigma_-\sigma_+) + i\Delta'[\sigma_-\sigma_+, \tilde{\rho}].
\end{aligned} \tag{51}$$

Given that $\sigma_+\sigma_- = 1/2(1 + \sigma_z)$ and $\sigma_-\sigma_+ = 1/2(1 - \sigma_z)$, then Eq. (51) turns into:

$$\dot{\tilde{\rho}} = -i\frac{1}{2}(2\Delta' + \Delta)[\sigma_z, \tilde{\rho}] + \frac{\gamma}{2}(\bar{n}+1)(2\sigma_-\tilde{\rho}\sigma_+ - \sigma_+\sigma_-\tilde{\rho} - \tilde{\rho}\sigma_+\sigma_-) + \frac{\gamma}{2}\bar{n}(2\sigma_+\tilde{\rho}\sigma_- - \sigma_-\sigma_+\tilde{\rho} - \tilde{\rho}\sigma_-\sigma_+). \tag{52}$$

Finally, in the Schrödinger picture:

$$\dot{\rho} = -i\omega_{A'}\frac{1}{2}[\sigma_z, \rho] + \frac{\gamma}{2}(\bar{n}+1)(2\sigma_-\rho\sigma_+ - \sigma_+\sigma_-\rho - \rho\sigma_+\sigma_-) + \frac{\gamma}{2}\bar{n}(\bar{n}+1)(2\sigma_+\rho\sigma_- - \sigma_-\sigma_+\rho - \rho\sigma_-\sigma_+), \quad (53)$$

where $\omega'_A = \omega_A + 2\Delta' + \Delta$ (the frequency shift: $\omega'_A - \omega_A$ is the so called Lamb shift). From looking at que equation, it can be seen that there exists a transition rate from the excited state to the ground one described by: $2\sigma_-\rho\sigma_+ - \sigma_+\sigma_-\rho - \rho\sigma_+\sigma_-$ (spontaneous emission) and another one in the opposite direction described by $2\sigma_+\rho\sigma_- - \sigma_-\sigma_+\rho - \rho\sigma_-\sigma_+$ (absorptive transition due to the existing thermal photong from the EM field). It must be noted that there is also a term equal to the former, accompanied by $\bar{n}$, which accounts for a stimulated transition due to thermal photons coming from the reservoir (EM field).

Finally, the master equations for the populations and coherences have been calculated:

$$\dot{\rho_{aa}} = \gamma(\bar{n}+1)\rho_{bb} - \gamma\bar{n}\rho_{aa}, \quad (54)$$

$$\dot{\rho_{ba}} = -i\omega_{A'}\rho_{ba} - \frac{\gamma}{2}(\bar{n}+1)\rho_{ba} - \frac{\gamma}{2}\bar{n}\rho_{ba} = -\rho_{ba}[i\omega_{A'} + \frac{\gamma}{2}(2\bar{n}+1)], \quad (55)$$

where a denotes the ground state and b the excited one. This system that has been considered could be an atom which is radiatively damped by its interaction with the many modes of an EM field in thermal equilibrium at temperature T.

2.2.1 Two state atom with non-radiative dephasing

In the previous case, we did not consider the fact that the interaction between the two level system and the EM field causes both energy loss from the atom, and damping of the atomic polarization (due to a randomization of the phases of the atom's wavefunctions by fluctuations of the field, which causes the overlap of the wavefunctions corresponding to the two levels to decay in time). That is why it is needed to account for additional dephasing interactions (coming from either elastic collisions or elastic phonon scattering in a solid).

We must now add a couple of terms to the Hamiltonian by assuming that we have two further reservoir interactions (they are not associated with additional radiated fields but simply modify the dynamics of the radiating source) given by: $H_{dephase} = H_{R_1} + H_{R_2} + H_{SR_1} + H_{SR_2}$, where each contribution can be seen below:

$$H_{R_1} + H_{R_2} = \sum_j \hbar\omega_{1j} r^\dagger_{1j} r_{1j} + \sum_j \hbar\omega_{2j} r^\dagger_{2r} r_{2j}, \quad (56)$$

$$H_{SR_1} + H_{SR_2} = \sum_{k,j} \hbar\kappa_{1jk} r^\dagger_{1j} r_{1k}\sigma_-\sigma_+ + \sum_{k,j} \hbar\kappa_{2jk} r^\dagger_{2j} r_{2k}\sigma_+\sigma_-. \quad (57)$$

Now, what it used to be called the reservoir $\mathcal{R}$, will now be called $\mathcal{R}_{12}$, and the whole reservoir will be $\mathcal{R} = \mathcal{R}_{12} \oplus \mathcal{R}_1 \oplus \mathcal{R}_2$. Each of these reservoir subsystems are assumed to be statistically independent.

Eq.(57) describes the scattering of quanta from the atom, either from $|1\rangle$ (H_{SR_1}) or from $|2\rangle$ (H_{SR_2}). They are virtual processes which scatter quanta with energy $\hbar\omega_{1k}$ and $\hbar\omega_{2k}$ into quanta with energy $\hbar\omega_{1j}$ and $\hbar\omega_{2j}$, so the state of the atom remains constant.

Just as the Hamiltonians in Eq.(56) show, they are equal to the Hamiltonian in Eq.(41). That is why for this system we will also keep the operators $\tilde{\Gamma}_1(t)$ and $\tilde{\Gamma}_2(t)$ seen in Eq.(25). These operators account for the interaction of the two level system with $\mathcal{R}_{12}$. Nevertheless, we are missing the interaction with $\mathcal{R}_1$ and $\mathcal{R}_2$. For this reason, the operators $\tilde{\Gamma}_3(t)$ and $\tilde{\Gamma}_4(t)$ will be introduced later on.

It must be noted that when Eq.(21) was derived, it was assumed that all the reservoir operators coupling to $\mathcal{S}$ had zero mean in the state R_0. However, in the case we are dealing with in this section, it no longer applies, just as it was mentioned above. The reservoir operators coupling to $\sigma_-\sigma_+$ and $\sigma_+\sigma_-$ in Eq.(57) have nonzero averages when $j = k$. That is why we will follow the procedure exposed in Eq.(16). Now, the unperturbed Hamiltonian will turn into $H'_S = \frac{1}{2}\hbar(\omega_A + \delta_p)\sigma_z$, where $\delta_p = \sum_j(\kappa_{2jj}\bar{n}_{2j} - \kappa_{1jj}\bar{n}_{1j}) = \int_0^\infty d\omega[g_2(\omega)\kappa_2(\omega) - g_1(\omega)\kappa_1(\omega)]\bar{n}(\omega, T)$.

This way, Hamiltonians in Eq.(57) turn into:

$$H'_{SR_1} + H'_{SR_2} = \sum_{k,j} \hbar\kappa_{1jk}(r^\dagger_{1j}r_{1k} - \delta_{jk}\bar{n}_{1j})\sigma_-\sigma_+ + \sum_{k,j} \hbar\kappa_{2jk}(r^\dagger_{2j}r_{2k} - \delta_{jk}\bar{n}_{2j})\sigma_+\sigma_-, \tag{58}$$

where $\bar{n}_{1j} \equiv \bar{n}(\omega_{1j}, T)$ and $\bar{n}_{2j} \equiv \bar{n}(\omega_{2j}, T)$ are the mean occupation numbers for those modes in $\mathcal{R}$ with frequencies ω_{1j} and ω_{2j}, respectively.

The sum of H'_S and $H'_{SR_1} + H'_{SR_2}$ is equal to the sum of the Hamiltonians in Eq.(56) and Eq.(57). And now, just as it was previously explained, the operators $\in \mathcal{R}$ in Eq.(58) have zero mean. Consequently, we have solved the problem that arose and can proceed onto substituting the operators seen in Eq.(48) and these:

$$\tilde{s}_3(t) = \sigma_-\sigma_+; \tilde{s}_4(t) = \sigma_+\sigma_-; \quad \tilde{\Gamma}_3(t) = \sum_{j,\vec{k}} \kappa_{1j\vec{k}}(r^\dagger_{1j}r_{1k}e^{i(\omega_{1j}-\omega_{1k})t} - \delta_{j\vec{k}}\bar{n}_{1j}); \tilde{\Gamma}_4(t) = \sum_{j,\vec{k}} \kappa_{2j\vec{k}}(r^\dagger_{2j}r_{2k}e^{i(\omega_{2j}-\omega_{2k})t} - \delta_{j\vec{k}}\bar{n}_{2j}) \tag{59}$$

directly into Eq.(21). That way, after following a series of calculus (see pages 31-32 of [5]), the master equation for this system is obtained:

$$\dot{\rho} = -i\omega_{A'}\frac{1}{2}[\sigma_z, \rho] + \frac{\gamma}{2}(\bar{n}+1)(2\sigma_-\rho\sigma_+ - \sigma_+\sigma_-\rho - \rho\sigma_+\sigma_-) + \frac{\gamma}{2}\bar{n}(\bar{n}+1)(2\sigma_+\rho\sigma_- - \sigma_-\sigma_+\rho - \rho\sigma_-\sigma_+) + \\ + \frac{\gamma_p}{2}(\sigma_z\rho\sigma_z - \rho), \tag{60}$$

where $\omega_{A'} \equiv \omega_A + 2\Delta' + \Delta + \delta_p + \Delta_p$, with: $\Delta = \sum_\lambda P\int d^3k \frac{g(\vec{k})|\kappa(\vec{k},\lambda)|^2}{\omega_A - kc}$, $\Delta' = \sum_\lambda P\int d^3k \frac{g(\vec{k})|\kappa(\vec{k},\lambda)|^2}{\omega_A - kc}\bar{n}(kc, T)$ and

$$\Delta_p = P\int_0^\infty d\omega \int_0^\infty d\omega' \frac{g_2(\omega)g_2(\omega')|\kappa_2(\omega,\omega')|^2 - g_1(\omega)g_1(\omega')|\kappa_1(\omega,\omega')|^2}{\omega - \omega'}.$$

From the master equation, Eq.(60, we obtained the master equations for the populations and the coherences:

$$\dot{\rho_{aa}} = \gamma(\bar{n}+1)\rho_{bb} - \gamma\bar{n}\rho_{aa}, \tag{61}$$

$$\dot{\rho_{ba}} = -[i\omega_{A'} + \frac{\gamma}{2}(2\bar{n}+1)]\rho_{ba} - \gamma_p\rho_{ba} = -[i\omega_{A'} + \frac{\gamma}{2}(2\bar{n}+1) + \gamma_p]\rho_{ba}. \tag{62}$$

If we set $\gamma_p = 0$, we get the two level system about which we talked earlier. That is why from now onwards, we will only be dealing with this general case and simply set $\gamma_p = 0$ when needed.

3 Solution of the master equation for the equilibrium state (analitical solution)

Una vez obtenidas las ecuaciones maestras de los sistemas, procedemos a determinar la solución de las mismas en el estado de equilibrio, es decir, para $t \to \infty$. Estos resultados se obtendrán analíticamente.

In this section, the solutions for the master equations in the equilibrium state are calculated, i.e., for $t \to \infty$. It must be noted that independently on what the initial state of the system is, the equilibrium state will always be the same. That is why the initial state of the system will not be taken into account in this section.

3.1 Cavity mode

The solution of Eq. (36) corresponding to the equilibrium state ($\dot{\rho}_{nn} = 0$) can be calculated by a recurrence procedure. For this purpose, it will be equated to zero, after which we obtain:

$$\rho_{(n+1)(n+1)} = \frac{1}{(1+\bar{n})(1+n)}[(2\bar{n}n + \bar{n} + n)\rho_{nn} - n\bar{n}\rho_{(n-1)(n-1)}]. \tag{63}$$

Now, if all the populations ($n \in \mathbb{N}$) are calculated, a general expression for a given n can be obtained:

$$\rho_{nn} = \left(\frac{\bar{n}}{1+\bar{n}}\right)^n \rho_{00}. \tag{64}$$

In order to find out ρ_{00}, the normalization condition has to be imposed: $Tr(\rho) = 1$, which is shown below:

$$Tr(\rho) = 1 \Rightarrow \sum_n \rho_{nn} = 1 \Rightarrow \rho_{00} \sum_{n=0}^{\infty} \left(\frac{\bar{n}}{1+\bar{n}}\right)^n = 1 \Rightarrow \rho_{00} \frac{1}{1-\frac{\bar{n}}{1+\bar{n}}} = 1 \Rightarrow \rho_{00} = \frac{1}{1+\bar{n}}, \tag{65}$$

in which Eq.(64) has been used as well as the result: $\sum_{n=0}^{\infty} x^n = \frac{1}{1-x} / |x| < 1$. Therefore, Eq.(64) can be rewritten as:

$$\rho_{nn} = \left(\frac{\bar{n}}{1+\bar{n}}\right)^n \frac{1}{1+\bar{n}} = \frac{\bar{n}^n}{(1+\bar{n})^{n+1}}. \tag{66}$$

Furthermore, as $\bar{n}$ is given by:

$$\bar{n} = \frac{e^{-\frac{\hbar\omega_c}{\kappa_B T}}}{1 - e^{-\frac{\hbar\omega_c}{\kappa_B T}}}, \tag{67}$$

Eq. (66) will end up being:

$$\rho_{nn} = e^{-\frac{\hbar\omega_c n}{\kappa_B T}} \left(1 - e^{-\frac{\hbar\omega_c}{\kappa_B T}}\right). \tag{68}$$

Eq.(68) represents the asintotic probability for the level n to be populated (P_n), that is, the probability of it being populated at $t \to \infty$ ($\dot{P}_n = 0$).

Having got this result is very useful, since it will allow us to check whether the average value of the $\hat{n}$ operator ($\langle a^+ a \rangle$) coincides with the number of photons within the reservoir ($\bar{n}$). This can be shown here:

$$\langle \hat{n} \rangle = Tr(\rho a^+ a) = \sum_n \langle n | \rho a^+ a | n \rangle = \sum_n n \rho_{nn} \Rightarrow \langle \hat{n} \rangle = \sum_n n e^{-\frac{\hbar\omega_c n}{\kappa_B T}} \left(1 - e^{-\frac{\hbar\omega_c}{\kappa_B T}}\right) = \left(1 - e^{-\frac{\hbar\omega_c}{\kappa_B T}}\right) \frac{e^{\frac{\hbar\omega_c}{\kappa_B T}}}{\left(e^{\frac{\hbar\omega_c}{\kappa_B T}} - 1\right)^2} \Rightarrow$$

$$\langle \hat{n} \rangle = \frac{e^{-\frac{\hbar\omega_c}{\kappa_B T}}}{\bar{n}} \frac{e^{\frac{\hbar\omega_c}{\kappa_B T}}}{\left(e^{\frac{\hbar\omega_c}{\kappa_B T}} - 1\right)^2} = \frac{1}{\bar{n}} \frac{1}{(1/\bar{n})^2} = \bar{n}, \tag{69}$$

where the result $\sum_n n e^{-xn} = \frac{e^{xn}}{(-1+e^{xn})^2}$ has been used and the expression for $\bar{n}$ (see Eq.(67)) has been kept in mind.

3.2 Two state atom with non-radiative dephasing

The equilibrium state is reached at $t \to \infty$ and can be calculated by setting $\dot{\rho_{aa}} = 0$ and $\dot{\rho_{ba}} = 0$, for which we will resort to Eq. (61) and Eq.(62). This way, we get:

$$\dot{\rho_{aa}} = 0 \Rightarrow (\bar{n}+1)\rho_{bb} = \bar{n}\rho_{aa} \Rightarrow (\bar{n}+1)(1-\rho_{aa}) = \bar{n}\rho_{aa} \Rightarrow \rho_{aa} = \frac{\bar{n}+1}{2\bar{n}+1} \quad \wedge \quad \rho_{bb} = \frac{\bar{n}}{2\bar{n}+1}, \tag{70}$$

and

$$\dot{\rho_{ba}} = 0 \Rightarrow -[i\omega_{A'} + \frac{\gamma}{2}(2\bar{n}+1) + \gamma_p]\rho_{ba} = 0 \Rightarrow \rho_{ba} = 0, \tag{71}$$

where we have kept in mind that $\rho_{aa} + \rho_{bb} = 1$.

4 Time evolution of the systems (analitical and numerical solutions)

A continuación se procederá a determinar la evolución temporal de los sistemas en cuestión. Para ello, se recurrirá a las ecuaciones maestras. En el caso del sistema de dos niveles, este procedimiento se podrá llevar a cabo tanto analítica como numéricamente (los resultados numéricos serán obtenidos usando Mathematica, de Wolfram Alpha). Sin embargo, en el caso del "cavity mode" tan solo se podrá realizar numéricamente.

In this section, the time evolution of the systems is obtained. In the case of the cavity mode, it will only be determined numerically with Mathematica. The reason is that the analitical solution would take very long to be calculated was the dimension of the system to be bigger than five. Nevertheless, in the case of the two level system with non radiative dephasing, not only will the solution be calculated analitically, but also numerically.

In this case, the initial state of the system will determine its time evolution. That is why it will be highlighted before giving any solution.

4.1 Cavity mode

Even though the exact analitical solution for Eq. (35) will not be obtained, just as it was mentioned above, let us choose a certain initial state of the system in order to see how it evolves with time, which will be plotted in Figure 4. It must be pointed out that from now onwards, all Figures concerning the cavity mode time evolution will contain legends in which the density matrix elements will be labelled as ρ_{ij}, where $|i\rangle$ and $|j\rangle$ actually refer to the $|i-1\rangle$ and $|j-1\rangle$ levels, respectively, of the cavity mode. For instance, the ground state will be labelled by ρ_{11} rather than: ρ_{00}.

Let us chose, for instance, the following initial mixed state: $|\psi(0)\rangle = \sqrt{0.4}\,|3\rangle + \sqrt{0.6}\,|4\rangle$ and the values: $\kappa = 0.3$, $\omega_{C'} = 0.5$ and $\bar{n} = 6$. If we look at the left hand graph of Figure 4, it is clear how at $t = 0$, all states are empty except for the third and fourth excited states (ρ_{44} and ρ_{55}), just as expected. The third excited one is initially at 0.4 and the fourth at 0.6. As time goes by, they start decaying, while those levels which are closer to the aforementioned ones that have higher energies (fifth -ρ_{66}- and sixth excited -ρ_{66}- ones), as well as those with lower energy than the third excited state go populating and then decay progresively. The ninth excited state (the last one considered) does not practically populate. Finally, it is the ground state

the one that keeps a higher population. The more excited the state, the less populated it will be. If we now focus on the coherences, it can be seen that only ρ_{45} and ρ_{54} are populated at $t = 0$ (at $0.49 \simeq \sqrt{0.4 \cdot 0.6}$), and then decay. Meanwhile, other coherences populate slighlty, though all of them tend to zero.

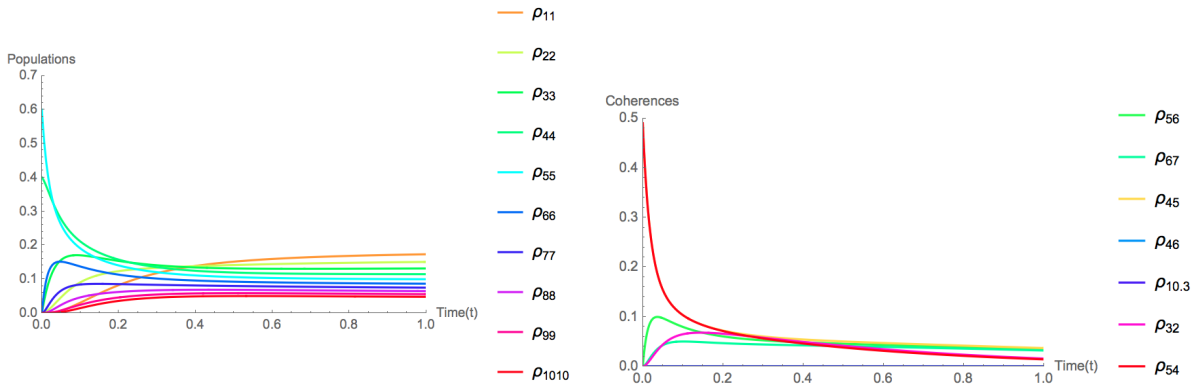

Figure 4: Density matrix elements behaviour with time for a cavity mode driven by thermal light. In this case, we have set $\kappa = 0.3$, $\omega_{C'} = 0.5$ and the number of photons in the EM field being 6. The initial state of the system is: $|\psi(0)\rangle = \sqrt{0.4}\,|3\rangle + \sqrt{0.6}\,|4\rangle$.

Furthermore, if the dimension of the considered subspace is increased, we get what can be seen in Figures 8, 9, 10 and 11. These Figures will be analised in Section 5, since the initial state used in those cases is a coherent state, which will be defined in Subsection 5.2. Having chosen this initial state is the reason why the dimension of the subspace has had to be increased, just to get the system to converge.

4.2 Two state atom in thermal equilibrium with non-radiative dephasing

4.2.1 Analitical solution

It has been obtained by two different procedures. On the one hand, I have calculated it myself for any initial state. On the other hand, analitical solutions have been obtained with Mathematica for a certain initial state. In order to check that both solutions are equal, the initial state used to determine the latter solution will be imposed in the former.

First of all, the derivation I obtained is the following. As for the populations, exact solutions can be obtained for Eq. (61), as it is shown below:

$$\begin{aligned} \frac{d\rho_{aa}}{\bar{n}+1-(2\bar{n}+1)\rho_{aa}} = \gamma dt \Rightarrow ln|\bar{n}+1-(2\bar{n}+1)\rho_{aa}| = -(2\bar{n}+1)\gamma t + lnC \Rightarrow \\ \Rightarrow \bar{n}+1-(2\bar{n}+1)\rho_{aa} = Ce^{-(2\bar{n}+1)\gamma t} \Rightarrow \\ \Rightarrow \rho_{aa} = \frac{-Ce^{-(2\bar{n}+1)\gamma t}}{2\bar{n}+1} + \frac{\bar{n}+1}{2\bar{n}+1} \wedge \rho_{bb} = \frac{Ce^{-(2\bar{n}+1)\gamma t}}{2\bar{n}+1} + \frac{\bar{n}}{2\bar{n}+1}, \end{aligned} \tag{72}$$

keeping in mind that $\rho_{aa} + \rho_{bb} = 1$, and where C has been introduced as an arbitrary constant.

As for the solution for the coherences (Eq. (62)) see:

$$\rho_{ba} = C' e^{-[i\omega_{A'} + \frac{\gamma}{2}(2\bar{n}+1)+\gamma_p]t}, \tag{73}$$

for which the same procedure as in Eq.(72) has been followed, and where C' has been introduced as an arbitrary constant.

Secondly, by setting as initial state that in which the system is in the excited state, the solution for Eq. (60)obtained with Mathematica is the following:

$$\rho_{aa}(t) = -\frac{(-1+e^{(-1-2\bar{n})t\gamma)}(1+\bar{n})}{1+2\bar{n}}; \qquad \rho_{bb}(t) = \frac{e^{(-1-2\bar{n})t\gamma}+\bar{n}+e^{(-1-2\bar{n})t\gamma}\bar{n}}{1+2\bar{n}}; \qquad \rho_{ab}(t) = \rho_{ba}(t) = 0 \tag{74}$$

Now, if we set the initial condition posed above ($\rho_{aa} = \rho_{ab} = \rho_{ba} = 0 \quad \wedge \rho_{bb} = 1$) in Eq.(72) and Eq.(73), we can verify that we obtain the same results as those in Eq.(74). For this purpose, we have calculated the constants C and C':

$$\rho_{aa}(0) = 0 \Rightarrow 0 = \frac{-C}{2\bar{n}+1} + \frac{\bar{n}+1}{2\bar{n}+1} \Rightarrow C = \bar{n}+1 \qquad or \qquad \rho_{bb}(0) = 1 \Rightarrow 1 = \frac{C}{2\bar{n}+1} + \frac{\bar{n}}{2\bar{n}+1} \Rightarrow C = \bar{n}+1$$
$$\rho_{ba}(0) = 0 \Rightarrow 0 = C', \tag{75}$$

and substituted them in Eq.(72) and Eq.(73).

4.2.2 Numerical solutions

The numerical solutions for the master equation Eq.(60)are plotted in Figure 5. We have set $\gamma = 0.3$, $\omega_{A'} = 0.5$, $\gamma_p = 3$ and have varied the number of photons in the electromagnetic field. Furthermore, the initial state has been choses as being: $|\psi(0)\rangle = \sqrt{0.8}\,|a\rangle + \sqrt{0.2}\,|b\rangle$ which, as the initial state of the density matrix is:

$$\rho(0) = \begin{bmatrix} 0.8 & \sqrt{0.8 \cdot 0.2} \\ \sqrt{0.8 \cdot 0.2} & 0.2 \end{bmatrix}, \tag{76}$$

If we have a look at Figure 5, except for the graph in the left top corner, it can be seen that in the equilibrium state, both levels end up being equally populated. In addition to this, the higher the amount of photons in the reservoir is, the quicker the system converges to the equilibrium state. What's more, the higher the amount of photons in the reservoir is, the more similar the levels are as far as their population is concerned. By looking at the graphs, it can be seen that the ground state's initial state is in 0.8 (just as we mentioned above), and that for the excited one is: 0.2. Furthermore, the initial state for the coherences is: 0.4 ($\sqrt{0.8 \cdot 0.2} = 0.4$).

As for the graph in the left top corner, as $\bar{n} = 1$, then the populations remain practically unperturbed and it could be stated that they nearly keep the same population as at the beginning. The coherences decay to zero, though much slower than in the other cases.

If we set $\gamma_p = 0$, then we get the numerical solutions for the master equation Eq.(53), which are plotted in Figure 6. We have set $\gamma = 0.3$, $\omega_{A'} = 0.5$ and have varied the number of photons. If we have a look at Figure 6,the same result is obtained: the time it takes the system to converge to the equilibrium state varies according to the number of photons in the reservoir.

If we now compare Figures 5 and 6, populations behave in the same way, from which it can be concluded that the non radiative dephasing term (that multiplied by γ_p) does not affect populations. Nevertheless,

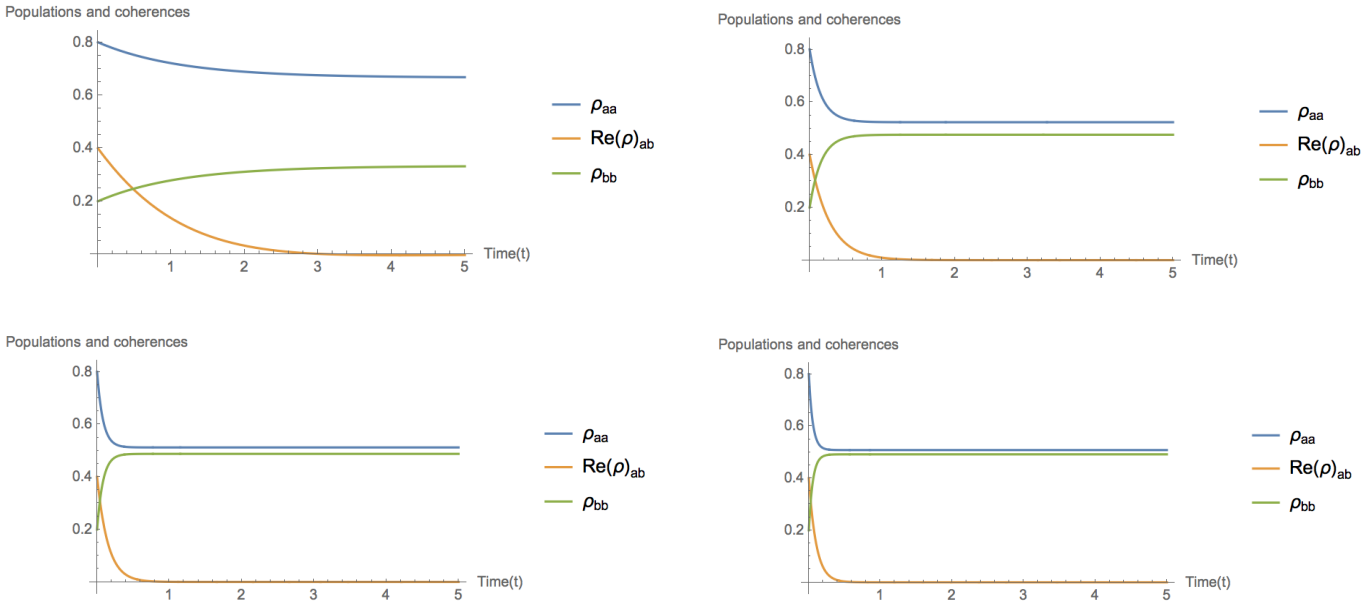

Figure 5: Density matrix elements behaviour with time. In this case, we have set $\gamma = 0.3$, $\omega_{A'} = 0.5$, $\gamma_p = 3$ and the number of photons in the EM field has been chosen as being: 1, 10, 20 and 30 (the corresponding graphs are those from the top left corner to the bottom right corner). The initial state is: $|\psi(0)\rangle = \sqrt{0.8}\,|a\rangle + \sqrt{0.2}\,|b\rangle$.

it does affect coherences. The non-radiative dephasing induces them to decay quicker. For instance, let us look at the graphs corresponding to $\bar{n} = 1$. While in the case of $\gamma_p = 3$, $Re(\rho_{ab})$ reaches the zero value at approximately $t \sim 2.2$, for $\gamma_p = 0$ it does so at $t \sim 3$. In addition to this, as the number of photons increases, the effect of the non-radiative dephasing term loses importance.

Now, let us check whether these results for $t \to \infty$ correspond to the expected ones, i.e., whether they comply the analitical results obtained for the equilibrium state, which are seen in Eq.(70) and Eq.(71). These is applicable independtly on the value of γ_p. For instance, let us consider the case of $\bar{n} = 1$. According to Eq.(70), the ground state (ρ_{aa}) should tend to ~ 0.67 while the excited one (ρ_{bb}) to ~ 0.33 and, as for the coherences, according to Eq.(71), they should all tend to zero. If we have a look at Figures 6 and 5, it can be seen that the numerical results comply the analitical ones. Let us now check it for another case, such as $\bar{n} = 30$. The ground state should tend to ~ 0.51 while the excited one to ~ 0.49, which is clearly seen in Figures 6 and 5.

5 Study of the effect of an external electric field over a harmonic oscillator driven by thermal light

Este apartado se centrará en el "cavity mode", aunque sometiéndolo a un campo eléctrico externo. Además, se introducirán varios conceptos nuevos que nos permitirán poder hacer un análisis más exhaustivo de este sistema. En primer lugar, se definirán los estados coherentes, lo que nos permitirá introducir a continuación

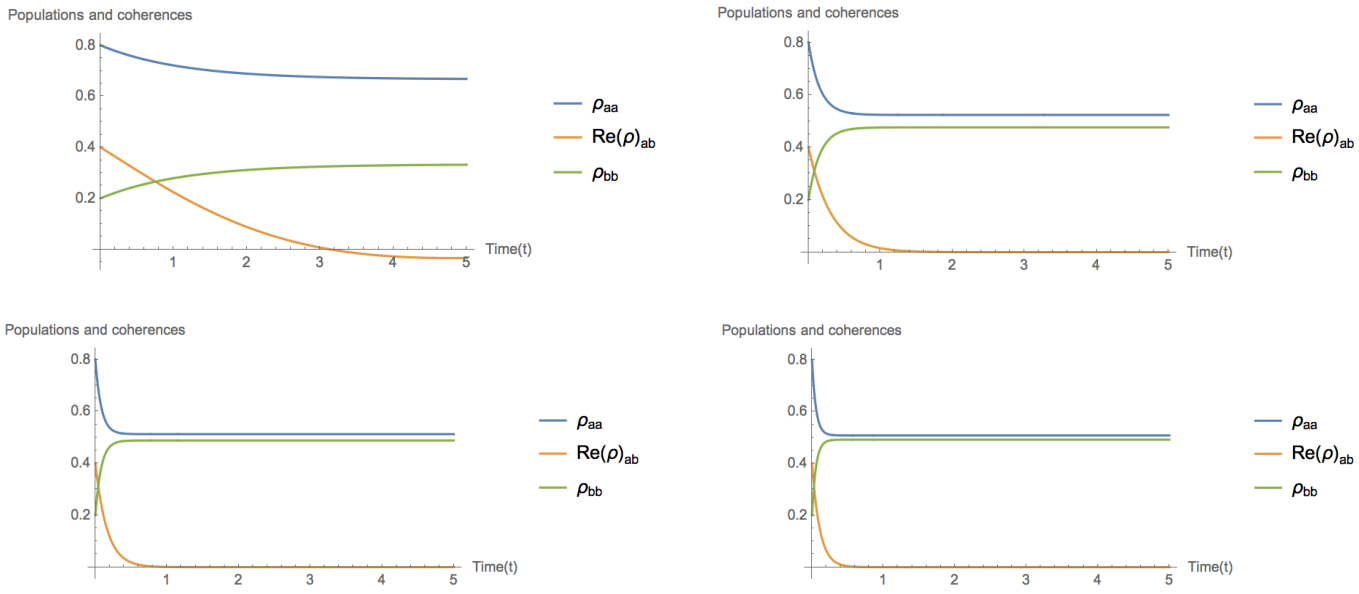

Figure 6: Density matrix elements behaviour with time. In this case, we have set $\gamma = 0.3$, $\omega = 0.5$, $\gamma_p = 0$ and the number of photons in the EM field has been chosen as being: 1, 10, 20 and 30 (the corresponding graphs are those from the top left corner to the bottom right corner). The initial state is: $|\psi(0)\rangle = \sqrt{0.8}\,|a\rangle + \sqrt{0.2}\,|b\rangle$.

una representación muy usada en óptica cuántica, la representación Q o de Husimi, ya que está definida en función de estos estados. Así pues, se procederá a resolver numéricamente la ecuación maestra de este último sistema. Esta solución se mostrará gráficamente mediante la representación de Husimi, así como la correspondiente al mismo sistema pero sin estar sometido al campo, el que ya se había analizado previamente, pero para subespacios más pequeños en secciones anteriores. De esta forma, se podrá determinar el efecto del campo al comparar ambas representaciones. Asimismo, se aprovechará este apartado para introducir una serie de gráficas que muestren la evolución de las poblaciones y coherencias de los dos sistemas. De esta forma, se podrá determinar el efecto del campo al comparar ambas representaciones, ya que con la función de Husimi no queda lo suficientemente claro.

In this section, a harmonic oscillator will be subjected to an electric field. In order to study this system, we will resort to the cavity mode driven by thermal light. The reason why we have used the words "harmonic oscillator" rather than "cavity mode" is that the latter is an electric field in itself, because of what it does not interact with any other electric field. Consequently, it might be paradoxical if we started studying the cavity mode assuming that it does interact with the external electric field. Nevertheless, the mathematical procedure will be the same, so that is why we will simply use the Hamiltonian for the cavity mode and then add a term that accounts for the external electric field. This addtional term will end up displacing the final state of the system from that we saw for the simple case of the cavity mode (this will be proved later on in this section).

Furthermore, the system's dynamics will be shown by using a representation known as the Husimi or Q-representation rather than the density matrix. This representation is obtained by using a certain set of states known as coherent states, which will be defined in Subsection 5.2.

5.1 Derivation of the master equation

In order to obtain the master equation for this system, an additional term will be added to the Hamiltonian of $\mathcal{S}$ (H_S), just as it was mentioned above: $\gamma\epsilon\hat{x} = \gamma\epsilon\sqrt{\frac{\hbar}{2m\omega}}(a^\dagger + a) \equiv \eta'(a^\dagger + a)$. Consequently, given that $\dot{\rho} = \frac{1}{i\hbar}[H_S, \rho]$, Eq. (35) will be transformed into:

$$\dot{\rho} = -i\omega_{c'}[a^\dagger a, \rho] - i\eta[a^\dagger + a, \rho] + \kappa(2a\rho a^\dagger - a^\dagger a\rho - \rho a^\dagger a) + 2\kappa\bar{n}(a\rho a^\dagger + a^+\rho a - a^\dagger a\rho - \rho a a^\dagger), \tag{77}$$

where $\eta \equiv \frac{\eta'}{\hbar}$.

The master equation for the populations is:

$$\begin{aligned}\dot{\rho}_{nn} =& \sqrt{n}\rho_{(n-1),n} + \sqrt{n+1}\rho_{(n+1),n} - \sqrt{n+1}\rho_{n,(n+1)} - \sqrt{n}\rho_{n,(n-1)} \\ &+ 2\kappa[(n+1)\rho_{(n+1)(n+1)}(1+\bar{n}) + \bar{n}n\rho_{(n-1)(n-1)} - (n + 2\bar{n}n + \bar{n})\rho_{nn}].\end{aligned} \tag{78}$$

In this case, the recurrence procedure we used in the simple case of the cavity mode is more complex, given that $\dot{\rho}_{nn}$ no longer depends just on populations, but also on coherences.

In order to prove that the final state of the system will remain the same though displaced, let us perform a unitary transformation to H_S. This will allow us to show that the new H_S still keeps the form of the Hamiltonian corresponding to a harmonic oscillator.

For this purpose, the displacement (unitary) operator is needed. This operator is defined as:

$$D(\alpha) \equiv e^{\alpha a^\dagger - \alpha^* a}, \tag{79}$$

and it has a very useful property: $D^\dagger(\alpha)aD(\alpha) = a + \alpha \Rightarrow D(\alpha)a^\dagger D^\dagger(\alpha) = a^\dagger + \alpha^*$ that will be used in the following procedure.[8]. Now, let us go onto the unitary transformation:

$$\begin{aligned}H'_S =& D^\dagger(\alpha_\eta)H_S D(\alpha_\eta) = \hbar\omega_c D^\dagger(\alpha_\eta)a^\dagger a D(\alpha_\eta) + \eta D^\dagger(\alpha_\eta)(a^\dagger + a)D(\alpha_\eta) \\ =& \hbar\omega_c D^\dagger(\alpha_\eta)a^\dagger D(\alpha_\eta)D^\dagger(\alpha_\eta)aD(\alpha_\eta) + \eta D^\dagger(\alpha_\eta)a^\dagger D(\alpha_\eta) + \eta D^\dagger(\alpha_\eta)aD(\alpha_\eta) \\ =& \hbar\omega_c(a^\dagger + {\alpha_\eta}^*)(a + \alpha_\eta) + \eta(a^\dagger + {\alpha_\eta}^* + a + \alpha_\eta) \\ =& \hbar\omega_c(a^\dagger a + a^\dagger\alpha_\eta + a{\alpha_\eta}^* + |\alpha_\eta|) + \eta(a^\dagger + {\alpha_\eta}^* + a + \alpha_\eta) \\ =& \hbar\omega_c a^\dagger a + a^\dagger(\hbar\omega_c\alpha_\eta + \eta) + a((\hbar\omega_c{\alpha_\eta}^* + \eta) + \hbar\omega_c|\alpha_\eta| + \eta\alpha_\eta,\end{aligned} \tag{80}$$

where the identity: $D(\alpha)D^\dagger(\alpha) = \mathbb{I}$ has been introduced. By choosing $\eta = -\hbar\omega_c\alpha_\eta$ and assuming that $\alpha_\eta = {\alpha_\eta}^*$, we finally get that Eq.(80) turns into

$$H'_S = \hbar\omega_c a^\dagger a, \tag{81}$$

proving that the system will still behave as a harmonic oscillator, though being displaced: $\alpha_\eta = -\frac{\eta}{\hbar\omega_c}$.

It must be kept in mind that each state of the present harmonic oscillator will be a linear combination of states of the previous, since the other's basis is the one that has been used. For instance, the ground state of the present harmonic oscillator might have a 90% of probability of being in the ground state of the previous, 5% of being in this latter's first excited state and so on.

5.2 Coherent States

A coherent state is defined as the eigenstate of the annhilation operator: $a|\alpha\rangle = \alpha|\alpha\rangle$ for a single mode, where $\alpha \in \mathbb{C}$. This can be proved as follows:

$$a|\alpha\rangle = e^{\frac{-|\alpha|^2}{2}} \sum_{n=0}^{\infty} \frac{\alpha^n}{\sqrt{n!}} \sqrt{n}\,|n-1\rangle = e^{\frac{-|\alpha|^2}{2}} \sum_{n=0}^{\infty} \frac{\alpha^n}{\sqrt{(n-1)!}}\,|n-1\rangle$$
$$m \equiv n-1 \Rightarrow a|\alpha\rangle = e^{\frac{-|\alpha|^2}{2}} \sum_{n=0}^{\infty} \frac{\alpha^{m+1}}{\sqrt{m!}}\,|m\rangle = \alpha|\alpha\rangle\,. \tag{82}$$

Furthermore, coherent states can be expanded in terms of Fock operators:

$$|\alpha\rangle = e^{\frac{-|\alpha|^2}{2}} \sum_{n=0}^{\infty} \frac{\alpha^n}{\sqrt{n!}}\,|n\rangle\,, \tag{83}$$

which can be proved as seen below:

$$|\alpha\rangle = D(\alpha)|0\rangle$$
$$e^{\alpha a^\dagger}|0\rangle \simeq |0\rangle + \alpha|1\rangle + \frac{1}{2!}\sqrt{2}\,|2\rangle + ... + \frac{\alpha^n}{n!}\sqrt{n!}\,|n\rangle = |0\rangle + \alpha|1\rangle + \frac{1}{\sqrt{2}}|2\rangle + ... + \frac{\alpha^n}{\sqrt{n!}}|n\rangle = \sum_n \frac{\alpha^n}{\sqrt{n!}}|n\rangle$$
$$e^{-\alpha^* a}|0\rangle = 0 \Rightarrow D(\alpha)|0\rangle = e^{\frac{-|\alpha|^2}{2}} e^{\alpha a^+}|0\rangle = e^{\frac{-|\alpha|^2}{2}} e^{\alpha a^+}|0\rangle = e^{\frac{-|\alpha|^2}{2}} \sum_n \frac{\alpha^n}{\sqrt{n!}}|n\rangle = |\alpha\rangle\,, \tag{84}$$

where the displacement operator has been used, as well as a property for two given operators A and B: $e^{A+B} = e^A e^B e^{-\frac{1}{2}[A,B]}$. [1]

5.3 Numerical solutions

Let us now proceed on to showing the numerical results obtained for the master equation (Eq. (77)).

We have chosen a subspace of dimension ten and have set it to be in this initial mixed state: $|\psi(0)\rangle = \sqrt{0.4}\,|3\rangle + \sqrt{0.6}\,|4\rangle$. Furthermore, we have selected the values: $\kappa = 0.2$, $\omega_{c'} = 3$, $\bar{n} = 6$ and $\eta = 0.5$ in Eq.(77). This way, the evolution of the system has been plotted in Figure 7. In order to analyse this Figure, we will resort to part of the explanation given for the same system though not subjected to the electric field (Subsection 4.1), for which the chosen initial state was the same. Again, ρ_{44} is at 0.4 at $t = 0$ while ρ_{55} is at 0.6. Furthermore, as for the coherences, only ρ_{45} and ρ_{54} are initially populated around 0.49. In addition to this, just as in the previous case, it is the ground state that keeps the higher population at the equilibrium state. Nevertheless, if Figures 4 and 7 are compared, a clear distinction can be noticed. While populations do not oscillate in the former, they do in the latter due to the electric field. However, the oscillation diminishes as time goes by. As for the coherences, they do tend to zero again, though oscillating. Again, the oscillation diminishes with time.

In the following Subsection (Subsection 5.4), the chosen initial state of the system will be a coherent state. For this reason, in order to get the system to converge, the dimension of the subspace has been increased up to 20 (we have increased even further the dimension of the subspace in the programs used in order to check there is convergence with a dimension of 20 already). Its evolution can be seen in Figures 12, 13, 14 and 15, which will be analysed later on.

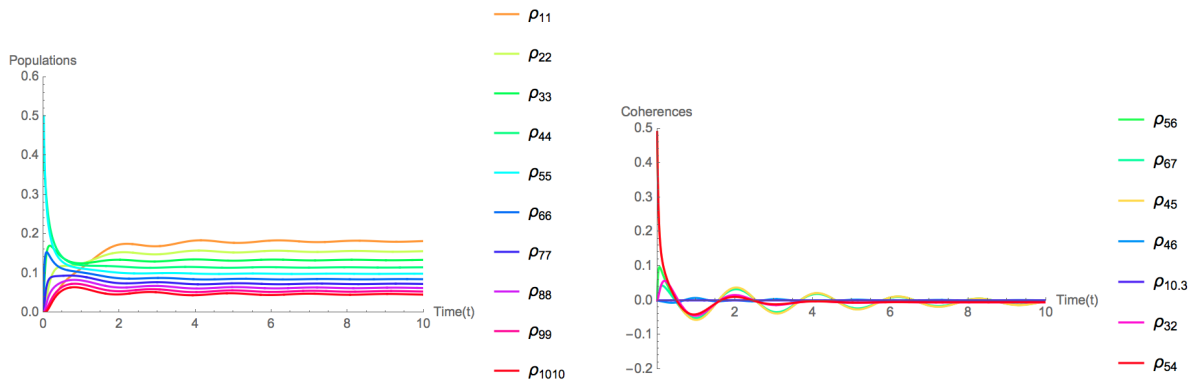

Figure 7: Density matrix elements behaviour with time for a cavity mode driven by thermal light subjected to an external electric field. $\kappa = 0.2$, $\omega_{c'} = 3$, $\bar{n} = 6$ and $\eta = 0.5$. The initial state of the system is: $|\psi(0)\rangle = \sqrt{0.4}\,|3\rangle + \sqrt{0.6}\,|4\rangle$.

5.4 Husimi representation (Q-representation)

In certain cases, describing a system using the Q-representation is more convenient than from its density matrix. Unlike the later (which is an operator), the Husimi representation is a quasiprobability function that represents the phase space distribution of a quantum state. It is commonly used in Quantum optics. [2]

It can be obtained from the elements of the density matrix, by averaging them in the coherent states basis:

$$Q(\alpha, \alpha^*) \equiv \frac{1}{\pi} \langle \alpha | \rho | \alpha \rangle \tag{85}$$

The Husimi representation is normalized:

$$Tr(\rho) = 1 \Rightarrow Tr\Big\{\frac{1}{\pi}\int d^2\alpha\, |\alpha\rangle \langle\alpha|\, \rho\Big\} = 1 \Rightarrow \frac{1}{\pi}\int d^2\alpha \langle\alpha|\, \rho\, |\alpha\rangle = \int d^2\alpha Q(\alpha, \alpha^*) = 1 \tag{86}$$

We will be using this representation to better understand the behaviour of the cavity mode driven by thermal light.

Since the solution for the density matrix has already been calculated, we can now determine $Q(\alpha, \alpha^*)$. For this purpose, the closing relation has been introduced twice (with two different indices, n and m). Furthermore, we have resorted to Eq.(83) in order to calculate $\langle m|\alpha\rangle$:

$$\langle m|\alpha\rangle = e^{\frac{-|\alpha|^2}{2}} \sum_{n=0}^{\infty} \frac{\alpha^n}{\sqrt{n!}} \delta_{nm} = e^{\frac{-|\alpha|^2}{2}} \frac{\alpha^m}{\sqrt{m!}}, \tag{87}$$

which is a result that will be required for the following procedure:

$$\begin{aligned} Q(\alpha, \alpha^*) &= \frac{1}{\pi} \sum_n \sum_m \langle\alpha|n\rangle \langle n|\, \rho\, |m\rangle \langle m|\alpha\rangle = \frac{1}{\pi} \sum_n \sum_m e^{\frac{-|\alpha|^2}{2}} \frac{(\alpha^*)^n}{\sqrt{n!}} \rho_{nm} e^{\frac{-|\alpha|^2}{2}} \frac{\alpha^m}{\sqrt{m!}} \\ &= \frac{1}{\pi} e^{-|\alpha|^2} \sum_n \sum_m \frac{(\alpha^*)^n \alpha^m}{\sqrt{n!m!}} \rho_{nm}, \end{aligned} \tag{88}$$

where $\langle n|\,\rho\,|m\rangle \equiv \rho_{nm}$.

This way, by replacing the elements of the density matrix that were obtained numerically, the Husimi representation for different times will be shown. The parameters of the system will be varied in order to see the differences. Not only will the cavity mode driven by thermal light subjected to the electric field will be represented, but also the system without being subjected to the electric field, in order to compare the effect of this field.

The cases that have been considered are seen in Table 1. It shows the values of the constants that have been substituted into Eq.(35) (in the first four cases) and into Eq. (77) (in the last four cases).

Case (Figures)		κ	$\bar{n}$	η
1	(16, 8)	0.5	0	0
2	(17, 9)	0	0	0
3	(18, 10)	0.5	6	0
4	(19, 11)	0	6	0
5	(20, 12)	0.5	0	0.5
6	(21, 13)	0	0	0.5
7	(22, 14)	0.5	6	0.5
8	(23, 15)	0	6	0.5

Tabla 1: Considered cases. Within the parenthesis of the first column, the references for the corresponding Figures to each case can be seen. The first reference alludes to the Husimi representation, while the second to a Figure where the time evolution of the populations and coherences is plotted.

At this point, there is a need to make a few comments regarding the distribution of some of the figures we will be analysing from now onwards, as well as the notation seen in some of them. First of all, those figures that show the Husimi representation of each case are at the end of this document. That is why it will be needed to resort to the final pages of it throughout the following analysis. Furthermore, it will be seen that in those figures that include the time evolution of populations and coherences, a rather misleading notation has been used. Populations are represented by: ρ_{ii} or ρ_{ijij}, while some coherences include a separation dot: $\rho_{j.mn}$, $\rho_{jm.n}$ or $\rho_{ij.mn}$. The reason is that in the case of coherences, was the dot not to be used, some ambiguity might arise regarding the levels between which the coherence is.

Let us start by analising Case 1 (Figures 8 and 16). In this case, the system is not subjected to the electric field. Let us focus on the initial state (t=0 in Figure 16). Just as it was mentioned above, the initial state is placed at $|\alpha_0\rangle = |1+3i\rangle$. There exists a coupling between the cavity and the reservoir, so that is why as time goes by, the initial state moves clockwise leading to the equilibrium state ($Re(\alpha) = Im(\alpha) = 0$), since $\bar{n} = 0$. Let us now go onto analysing Figure 8. As for the populations, it can be noticed that most of them are initially populated. Nevertheless, as time goes by, the highest excited levels decay, i.e., their populations go transferring to lower energy states progresively. Finally, it is the ground state the only one that remains populated. In fact, it keeps the total of the population while all the other states tend to zero. This is in accordance to the result obtained in Eq.(69). In this case, $\bar{n} = 0$ then, according to Eq.(69), $\langle\hat{n}\rangle$ (the average number of photons in the cavity) should be zero. This is satisfied given that there is only one level, among the twenty considered, that has a population of 1, while all the others are empty. Consequently, since that single level is the ground state, then $\langle\hat{n}\rangle = 0$. As for the coherences, it can be noticed that not only do they decay (due to the coupling with $\mathcal{R}$), but also they oscillate. The reason is that the state of the system is like: $|\psi(t)\rangle = \sum_{n=0}^{\infty} c_n(0)e^{-iE_nt/\hbar}\,|n\rangle$. Then, the density matrix: $\rho = |\psi(t)\rangle\langle\psi(t)| = \sum_{n=0}^{\infty}\sum_{m=0}^{\infty} c_n(0)c_m^*(0)e^{-i\omega_{nm}t}\,|n\rangle\langle m|$ $/\omega_{nm} \equiv (E_n - E_m)/\hbar$. Consequently, since

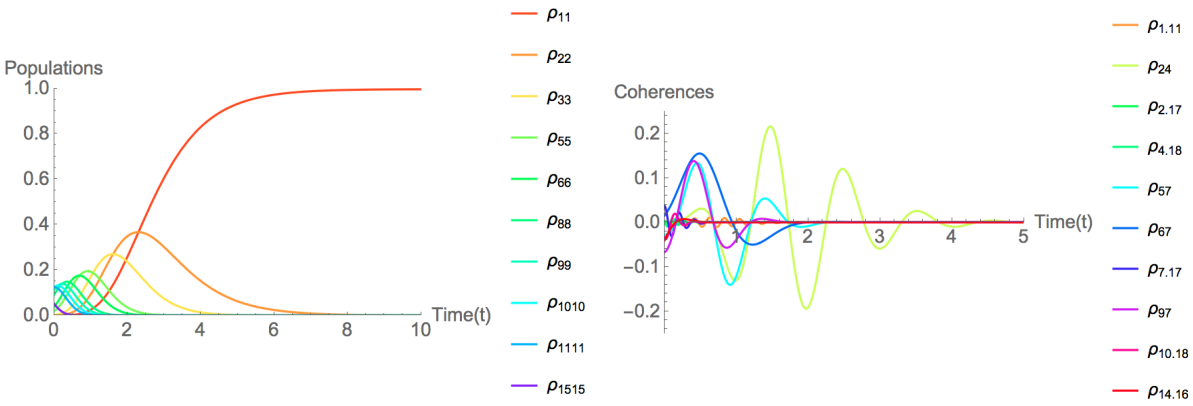

Figure 8: Representation of the populations and coherences for a cavity mode driven by thermal light where the parameters used are: $\kappa = 0.5$, $\omega_{C'} = 3$ and the reservoir is in the vacuum state ($\bar{n} = 0$). The initial state of the system is: $|\alpha_0\rangle = |1 + 3i\rangle$.

coherences generally comply: $E_n \neq E_m$ then, they will oscillate with the Bohr frequency ω_{nm}. Let us further analyse them. If we have a look at Figure 8 and focus on the time evolution of the coherence ρ_{67}, it is clear that its period is: $T \simeq 2$. It is known that the period is given by: $T = \frac{2\pi}{\omega}$. Consequently, $\omega \simeq 3.14$, which is pretty similar to the characteristic frequency of the cavity mode in this case: $\omega_{C'} = 3$. This is what we expected, since the coherence we are dealing with is that between two subsequent states, and ω represents the frequency of oscillation between two subsequent states. Furthermore, if we have a look at ρ_{57}, it is seen that its period is close to 1, which implies that $\omega \simeq 6.15$, which would be the double of the characteristic frequency, just as we expect for levels which are separated the double. In fact, if we have a look at coherence ρ_{97}, which represents the same distance between levels as ρ_{57}, it can be noticed that they oscillate with the same frequency. The more separeted the levels are (see coherences such as $\rho_{1.11}$), the quicker the oscillation is.

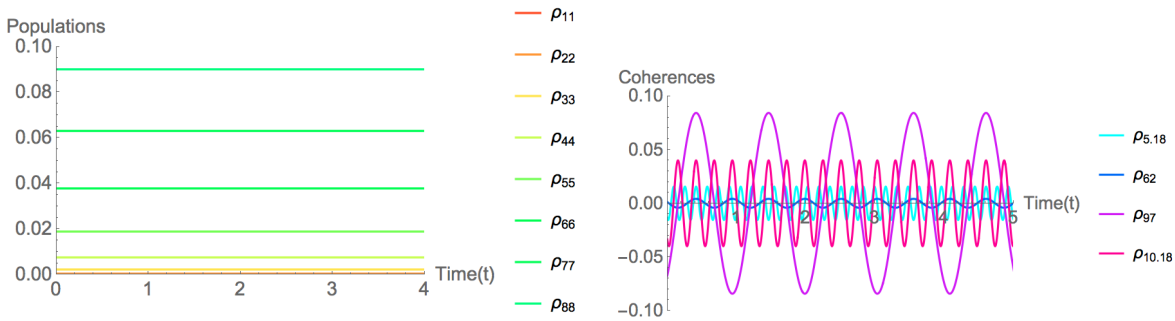

Figure 9: Representation of the populations and coherences for a cavity mode driven by thermal light where the parameters used are: $\kappa = 0$ (there is no coupling), $\omega_{C'} = 3$ and the reservoir is in the vacuum state ($\bar{n} = 0$). The initial state of the system is: $|\alpha_0\rangle = |1 + 3i\rangle$.

Now, let us consider Case 2 (Figures 9 and 17). Unlike Case 1, now there does not exist any coupling between the cavity and the reservoir. For this reason, as time goes by, if we have a look at Figure 17, the state

moves clockwise though remains describing a circle with the same radius, that is, it does not lead towards the center. Now, by looking at Figure 9, it can be seen that there is no crossing between states, which is due to the fact that in this case we are considering a closed system, so each level remains unperturbed. Again, by looking at the coherence ρ_{97}, it can be seen that $T \sim 1 \Rightarrow \omega \simeq 6.15$, which is similar to the frequency between levels $|n\rangle$ and $|n+2\rangle$. However, in this case, the non-coupling to the environment can be seen in the fact that the amplitude of the oscillations remains constant, unlike in Case 1. Furthermore, it can be seen that the frequency of oscillation of $\rho_{5.18}$ and ρ_{62} is the double to that with which $\rho_{10.18}$ and ρ_{62} oscillate, respectively. This can be explained in the same way as for Case 1.

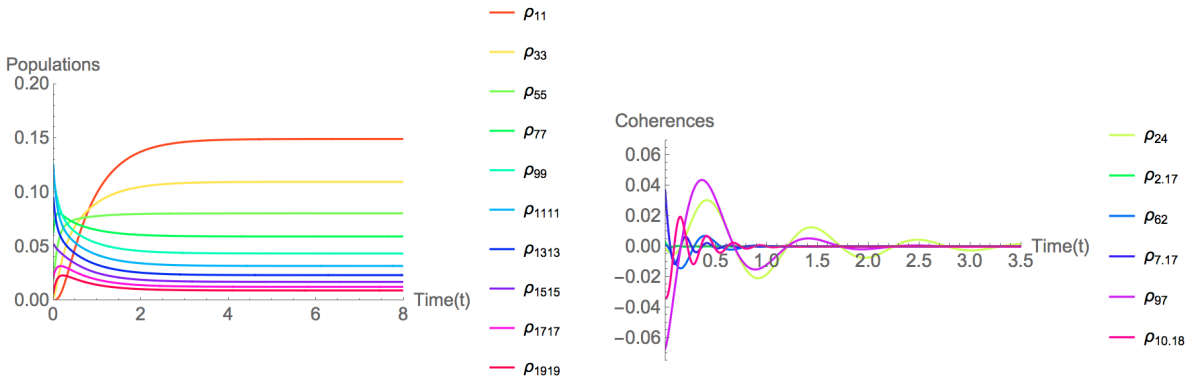

Figure 10: Representation of the populations and coherences for a cavity mode driven by thermal light where the parameters used are: $\kappa = 0.5$, $\omega_{C'} = 3$ and $\bar{n} = 6$. The initial state of the system is: $|\alpha_0\rangle = |1+3i\rangle$.

Let us go onto Case 3 (Figures 10 and 18). Again, in this case there is a coupling which induces the system to direct towards the center (just as in Case 1). Nevertheless, there is a remarkable difference and it is the fact that not only does it move spiraling towards the center, but also, it goes modifying its shape as time goes by. This is due to the fact that the reservoir is no longer in the vacuum, but has six photons. As it can be seen in Figure 18, at t=0, the state is exactly the same as in the previous cases, but then it goes progresively augmenting its radius. This implies that the population is evenly divided among many states. As for Figure 10, unlike Case 1, where all excited levels tended to zero independently on their initial state, all states remain populated. This is in accordance to Eq. (69), since $\bar{n} = 6$. The state that keeps the higher population is obviously the ground state. It can be seen that at $t = 0$, ρ_{1111} (the population corresponding to the $|n = 10\rangle$ level) has the higher population. In order to justify this result, we will perform $\frac{\mathrm{d}P_n}{\mathrm{d}n}$, where P_n is the probability of the $|n\rangle$ level to be populated, and then equate it to zero to find out what the value of n that makes P_n maximum is (n_m), i,e, what the level with higher population is:

$$\frac{\mathrm{d}P_n}{\mathrm{d}n} = e^{|\alpha|^2}\left[\frac{|\alpha|^{2n} ln(|\alpha|^2) n! - |\alpha|^{2n}\frac{\mathrm{d}n!}{\mathrm{d}n}}{(n!)^2}\right];$$
$$\left.\frac{\mathrm{d}P_n}{\mathrm{d}n}\right|_{n_m} = 0 \Rightarrow ln(|\alpha|^2) n_m! = \frac{\mathrm{d}n_m!}{\mathrm{d}n_m} \Rightarrow ln(|\alpha|^2) = \sum_i \frac{1}{n_m - i} \equiv f(n_m) \Rightarrow f^{-1}(|\alpha|^2) = n_m, \tag{89}$$

where the following result has been used: $\frac{\mathrm{d}n!}{\mathrm{d}n} = n_m! \sum_i \frac{1}{n_m - i}$. Let us substitute into $ln(|\alpha|^2) = \sum_i \frac{1}{n_m - i}$ the initial value of α (the initial coherent state used is: $|1+3i\rangle$), as well as perform the sum over the first six terms of the summatory (they are the most predominant ones):

$$ln(|1+3i|^2) \simeq \sum_{i=1}^{6} \frac{1}{n_m - i} \Rightarrow n_m \simeq 10. \tag{90}$$

The result seen in Eq. (90) already justifies the reason why the state with a higher population is $|10\rangle$. As for the coherences, again, the amplitude of oscillation goes decreasing. It can also be seen that coherences such as ρ_{24} and ρ_{97} oscillate with the same frecquency, just as it was expected.

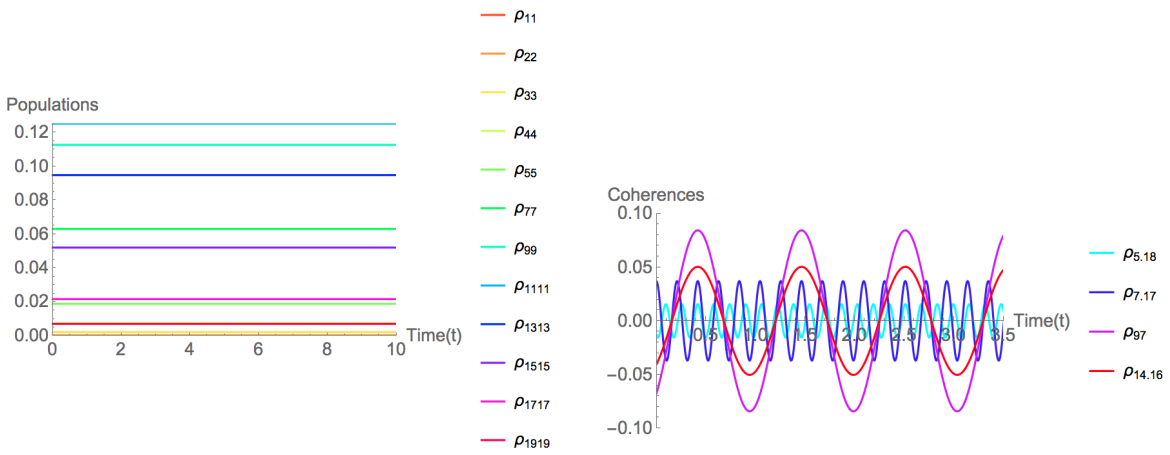

Figure 11: Representation of the populations and coherences for a cavity mode driven by thermal light where the parameters used are: $\kappa = 0$ (there is no coupling), $\omega_{C'} = 3$ and $\bar{n} = 6$. The initial state of the system is: $|\alpha_0\rangle = |1 + 3i\rangle$.

The final considered case which is not subjected to an electric field is Case 4 (Figures 11 and 19). Unlike Case 2, by looking at Figure 19 the shape goes modifying slightly due to the fact that $\bar{n} = 6$, though it does not lead towards the centre because of $\kappa = 0$ (no coupling). Now, let us look at Figure 11. Again, it is the $|10\rangle$ level that has a higher population, which remains constant, just as it was explained in Case 2, where no coupling exists either. Furthermore, the population of levels increases from the ground state to the ninth excited one, and then it decreases. As for the coherences, since there is no coupling, the amplitude of oscillation remains constant. Again, it can also be seen that coherences such as ρ_{97} and $\rho_{14,16}$ oscillate with the same frecquency, just as explained in previous cases.

Let us now begin analising the same systems described above, though subjected to the external electric field.

Once the unperturbed Hamiltonian of the cavity mode (H_0) is diagonalised, the eigenvalues of the system are like: $E_n^o = (\frac{1}{2} + n)\hbar\omega \quad /n \in \mathbb{N}$ with their corresponding eigenvectors: $\{|n^o\rangle\} \quad /n \in \mathbb{N}$. Nevertheless, when diagonalising the new Hamiltonian ($H_0 + V$, where V is a perturbation, the electric field), the eigenvalues will be: $E_n \quad /n \in \mathbb{N}$ with eigenvectors that will be linear combinations of the previous: $\{|n\rangle = \sum_m c_{n,m} |m^o\rangle\} \quad /n \in \mathbb{N}$, where $c_{n,m}$ are constant coefficients. Furthermore, if we resort to first order perturbation theory, our new eigenvectors will be like: $|n\rangle \simeq |n^o\rangle + \eta \sum_{p \neq n} \sum_i \frac{\langle p^{oi}|(a+a^\dagger)|n^o\rangle}{E_n^o - E_p^o} |p^{oi}\rangle$. For this reason, even the populations will be perturbed in such a way that they will oscillate.

Let us now go onto Case 5 (Figures 12 and 20) is the analogous to Case 1. No appreciable difference can be noticed between Figures 16 and 20. That is why we will resort to the analysis of the populations and coherences with time, so let us now compare Figures 8 and 12. As for the populations, the most affected ones by the electric field are those with lower energy, ranging from the ground state to the third excited state (ρ_{44} in Figure 12). They oscillate, though as time goes by, this effect diminishes and the equilibrium state ends up being the same in both cases. As for the coherences, even though they also tend to zero for $t \to \infty$, their

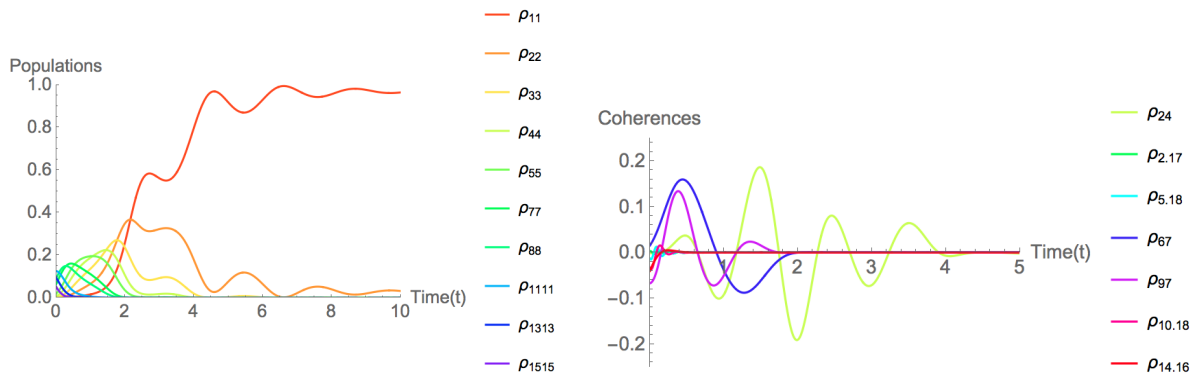

Figure 12: Representation of the populations and coherences for a cavity mode driven by thermal light subjected to an electric field, where the parameters used are:$\kappa = 0.5$, $\omega_{C'} = 3$, $\eta = 0.5$ and the reservoir is in the vacuum state ($\bar{n} = 0$). The initial state of the system is: $|\alpha_0\rangle = |1 + 3i\rangle$.

period varies. For instance, the coherence that was analised earlier on, ρ_{67}, had $T \sim 2$. In this case, again, $T \sim 2$, just as expected. The reason is that if we assume η as being small enough so as to use perturbation theory, the corrected energies will be: $E_n = E_n^o + \Delta E$, where, at first order: $\Delta E = \langle n|\eta(a^\dagger + a)|n\rangle = 0$. Consequently, since $E_n = E_n^o = \hbar\omega_{C'}(\frac{1}{2} + n)$ then the frecquency of oscillation is clearly not affected by the presence of the external electric field, just as the numerical solutions have shown.

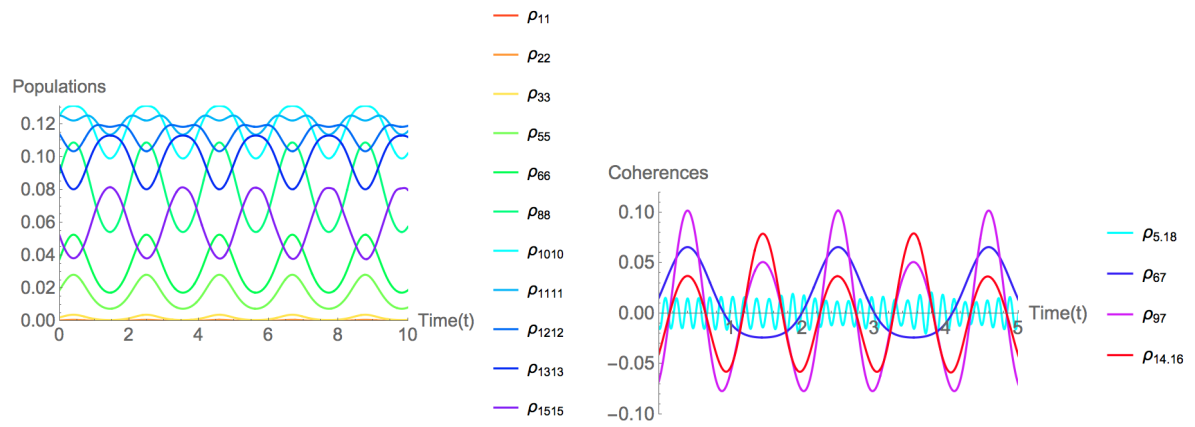

Figure 13: Representation of the populations and coherences for a cavity mode driven by thermal light subjected to an electric field, where the parameters used are:$\kappa = 0$, $\omega_{C'} = 3$, $\eta = 0.5$ and the reservoir is in the vacuum state ($\bar{n} = 0$). The initial state of the system is: $|\alpha_0\rangle = |1 + 3i\rangle$.

Let us now go onto Case 6 (Figures 9 and 13 will be compared). In this case, remarkable differences can be seen. As for the populations, while they do not cross in Figure 9, in the case in which the system is subjected to the electric field, they do, which is induced by the external field. Furthermore, in the latter case, not all of the populations oscillate in phase. From the ground state up to $|n = 9\rangle$ (ρ_{1010}), they oscillate in phase. Nevertheless, from ρ_{1111} there is a dephase and so, approximately from ρ_{1212} onwards, they oscillate in phase among them. As for the coherences, even though they oscillate in both cases, in Figure 13 they do

not keep a constant amplitude, unlike in Figure 9.

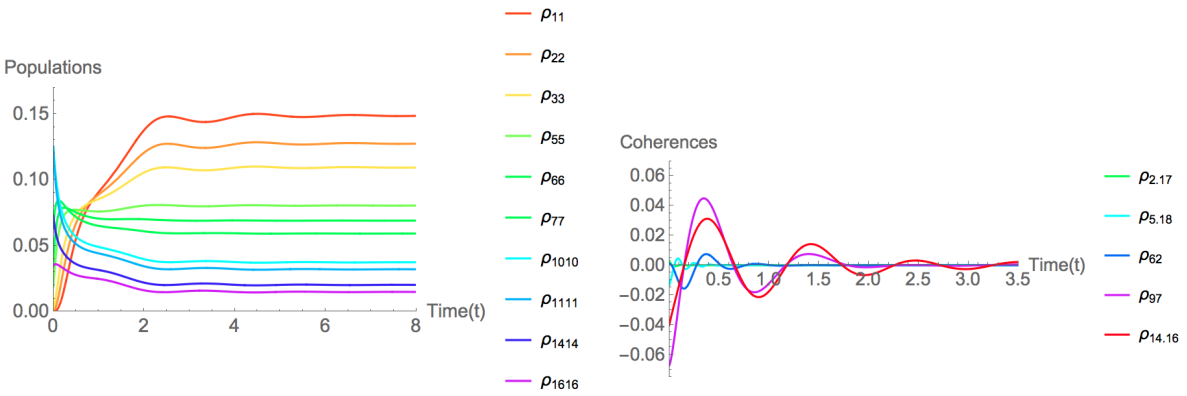

Figure 14: Representation of the populations and coherences for a cavity mode driven by thermal light subjected to an electric field, where the parameters used are:$\kappa = 0.5$, $\omega_{C'} = 3$, $\eta = 0.5$ and $\bar{n} = 6$. The initial state of the system is: $|\alpha_0\rangle = |1 + 3i\rangle$.

As for Case 7, let us now compare Figures 10 and 14. The same differences that were found between Cases 1 and 5 can be found between Case 3 and the one we are analising now.

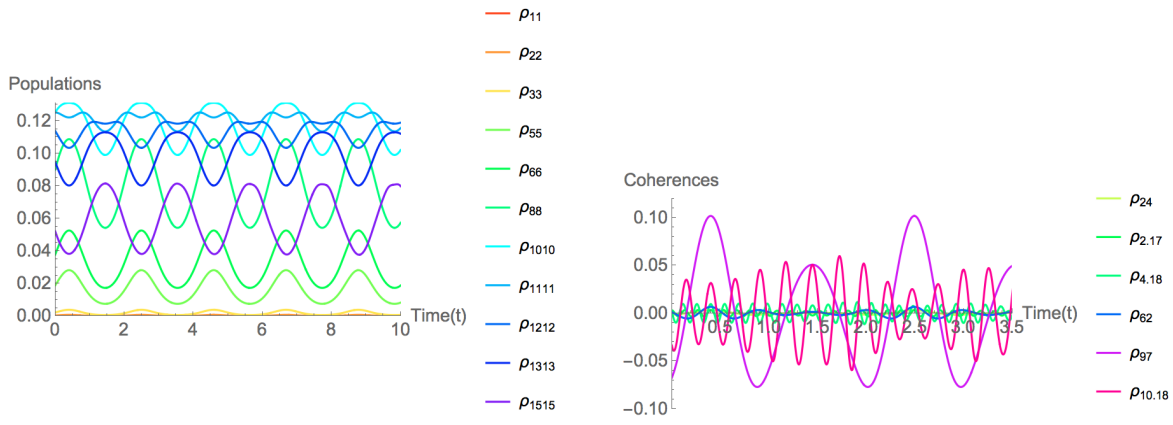

Figure 15: Representation of the populations and coherences for a cavity mode driven by thermal light subjected to an electric field, where the parameters used are:$\kappa = 0$ (no coupling), $\omega_{C'} = 3$, $\eta = 0.5$ and $\bar{n} = 6$. The initial state of the system is: $|\alpha_0\rangle = |1 + 3i\rangle$.

Finally, Case 8 will be analised by comparing Figures 11 and 15. There exists crossing between states, just as it was explained in Case 6. Furthermore, just as it could also be seen in Case 6, even though the amplitude of oscillation of the coherences does not diminish, it goes changing periodically.

6 Summary and conclusions

A lo largo de este trabajo se ha llegado a una serie de conclusiones que se enumerarán de nuevo en este apartado. En primer lugar, se ha verificado que los procesos de decoherencia provocan un decaimiento de los elementos no diagonales de la matriz densidad que describe algunos sistemas abiertos, tal y como se pretendía mostrar. Además, en el caso del "cavity mode" también se ha analizado el correspondiente cerrado ($\kappa = 0$), pudiendo ver que, efectivamente, sus coherencias permanecen constantes. Por otro lado, todas las soluciones numéricas están acorde con las analíticas, así como con la teoría subyacente.

Throughout this work, a series of conclusions have been reached that will be highlighted in this section. First of all, decoherence processes induce coherences to decay in the case of open systems, unlike what happens with closed systems. For the cavity mode driven by thermal light (we have set the coupling parameter between the system and the environment as: $\kappa \neq 0$), the analogous closed system has been analysed ($\kappa = 0$), from which we have conluded that unlike in the former case, in the latter, coherences remain constant. Secondly, it has been checked that all numerical solutions satisfy the analitical results obtained and the theory beneath it. In the case of the cavity mode driven by thermal light, the result $\langle \hat{n} \rangle = \bar{n}$ is satisfied for all cases. Furthermore, the frequency of oscillation of the coherences between two subsequent levels is the characteristic of the cavity mode. Finally, it has been obtained that the higher the difference between energy levels, the higher the frequency of oscillation, just as it was expected. As for the cavity mode driven by thermal light subjected to an external electric field, up to first order perturbation theory, the frequency of oscillation of the coherences is the same as in the unperturbed case. To conclude, we can summarize that by tracing over the reservoir's degrees of freedom, the entanglement between the environment and the system decays, which produces a decoherence process in the latter that we have been able to analise in a couple of systems.

References

[1] Orszag, M.(2008). States of the Electromagnetic Field I.*Quantum Optics. Including Noise Reduction, Trapped Ions, Quantum Trajectories, and Decoherence* (pp. 31-39). Berlin Heidelberg: Springer.

[2] Orszag, M.(2008). Phase Space Description.*Quantum Optics. Including Noise Reduction, Trapped Ions, Quantum Trajectories, and Decoherence* (pp. 73-75). Berlin Heidelberg: Springer.

[3] Orszag, M.(2008). Decoherence.*Quantum Optics. Including Noise Reduction, Trapped Ions, Quantum Trajectories, and Decoherence* (pp. 311-328). Berlin Heidelberg: Springer.

[4] Cohen-Tannoudji, C.,Dupont-Roc, J. and Crynberg,G. (2004). Radiation Cosidered as a Reservoir: Master Equation for the Particles.*Atoms-Photon interactions* (pp. 257-301). Weinheim: WILEY-VCH Verlag GmbH and Co. KGaA.

[5] Carmichael, H.(1991). *An Open Systems Approach to Quantum Optics*. Berlin Heidelberg: Springer.

[6] Zurek, W.H.(2002). Decoherence and the transition from Quantum to Classical - Revisited. *Los Alamos Science (27)*.

[7] Fujii K. (2014). Introduction to the Rotating Wave Approximation (RWA) : Two Coherent Oscillations *arχiv:1301.3585v3 [quant-ph]*[`https://arxiv.org/abs/1301.3585v3`]

[8] Gerry, C.C. and Knight P.L. (2005). *Introductory Quantum Optics*. New York: Cambridge University Press.

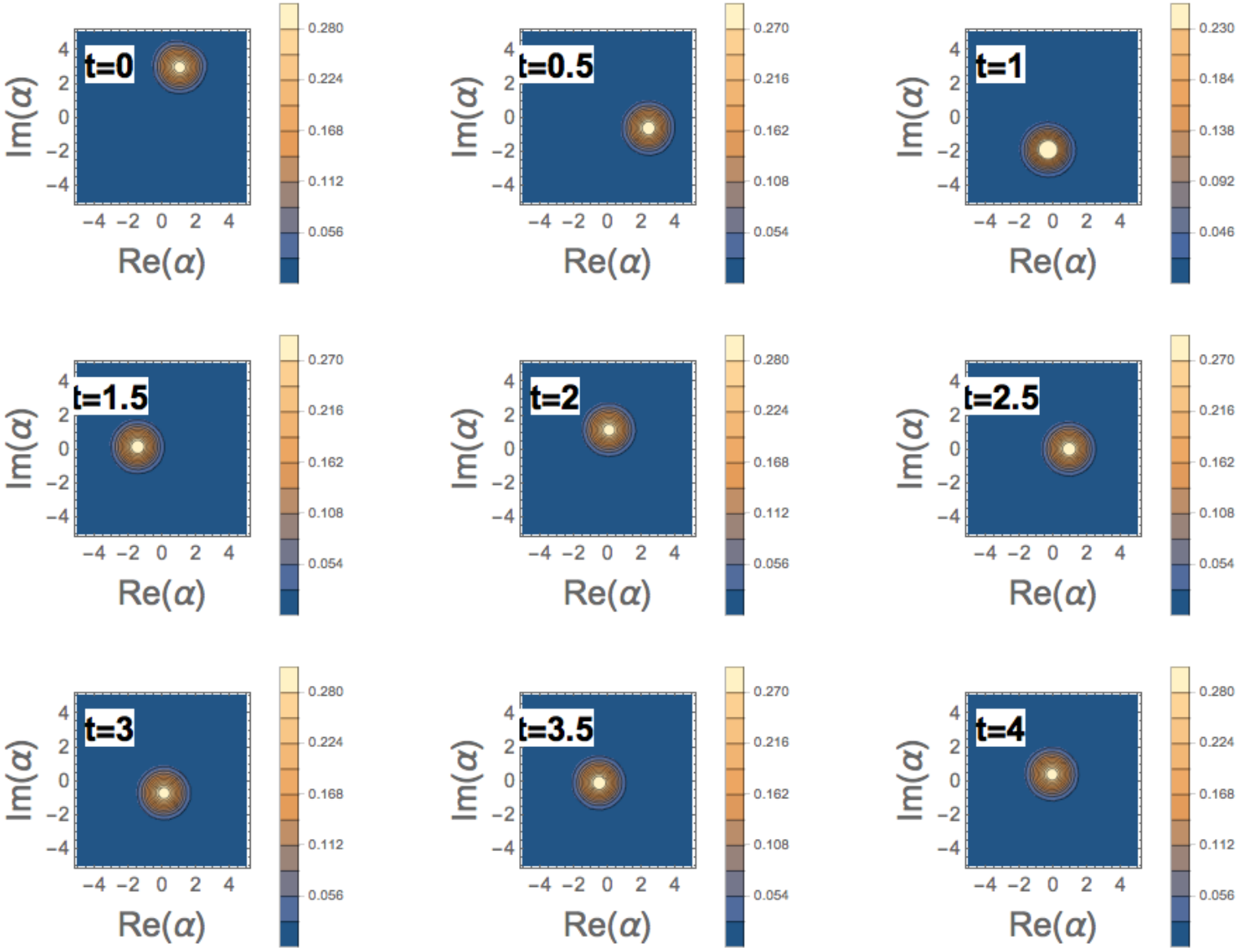

Figure 16: Husimi representation for a driven by thermal light where the parameters used are: $\kappa = 0.5$, $\omega_{C'} = 3$ and the reservoir is in the vacuum state ($\bar{n} = 0$). The initial state of the system is: $|\alpha_0\rangle = |1 + 3i\rangle$.

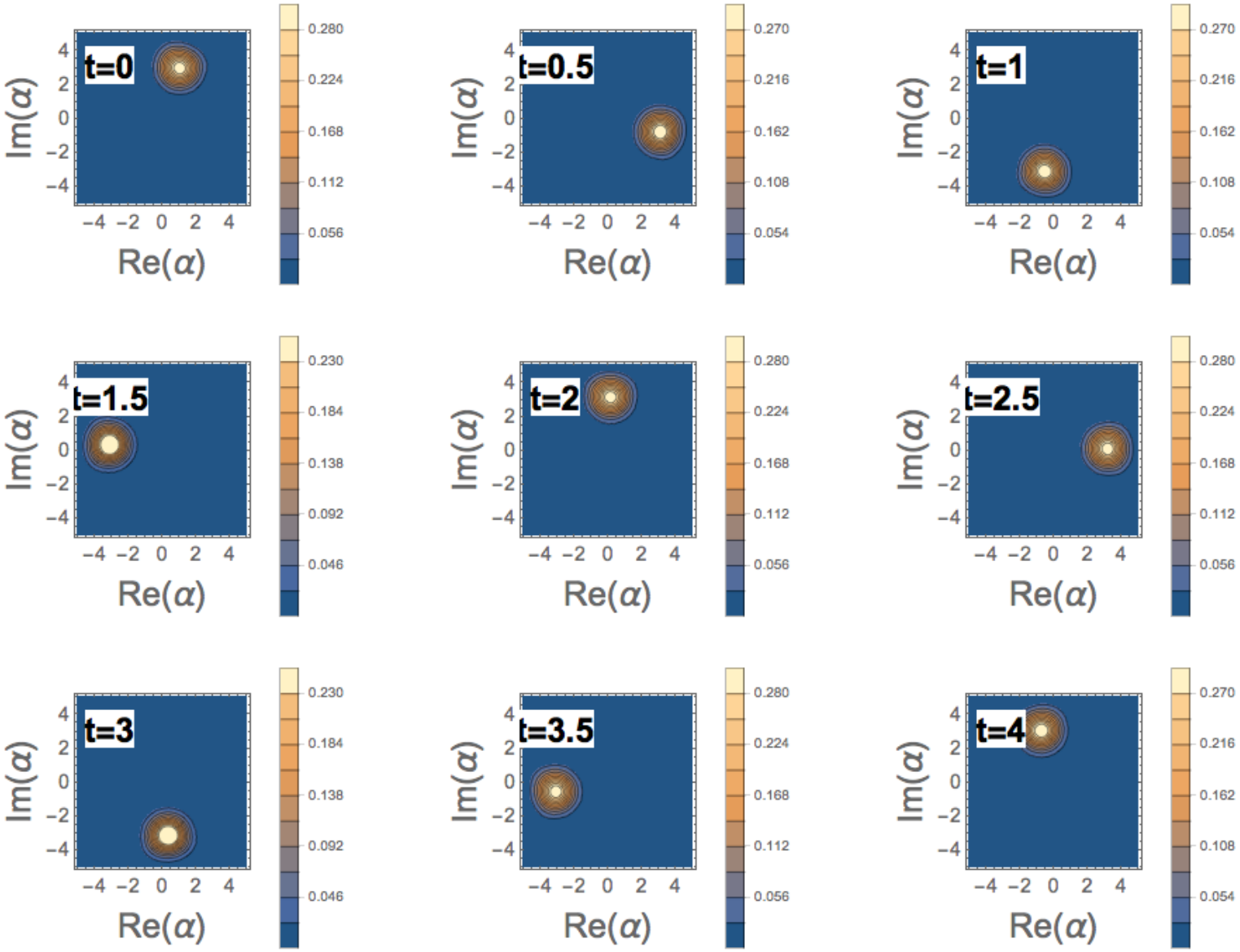

Figure 17: Husimi representation for a cavity mode driven by thermal light where the parameters used are: $\kappa = 0$ (there is no coupling), $\omega_{C'} = 3$ and the reservoir is in the vacuum state ($\bar{n} = 0$). The initial state of the system is: $|\alpha_0\rangle = |1 + 3i\rangle$.

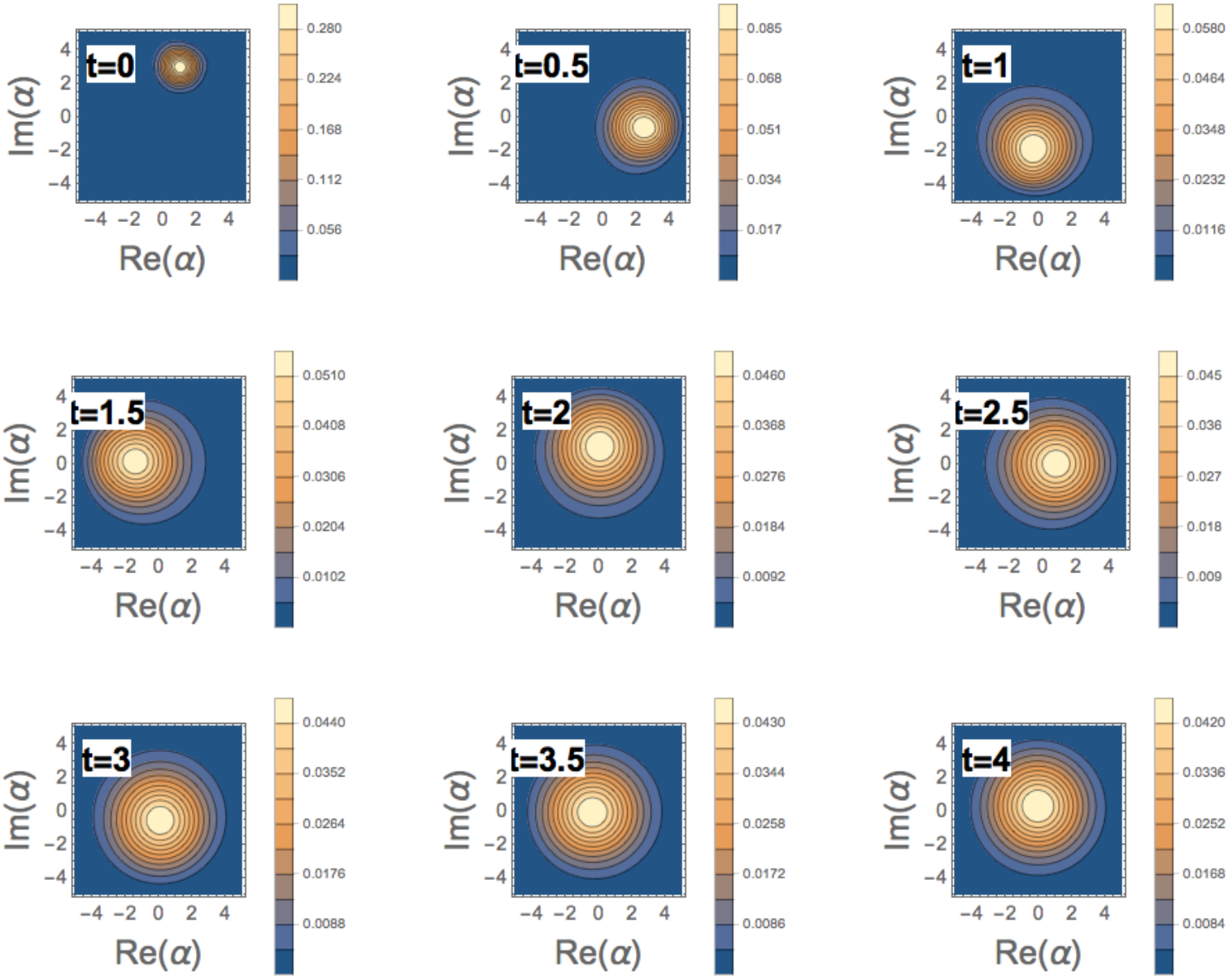

Figure 18: Husimi representation for a cavity mode driven by thermal light where the parameters used are: $\kappa = 0.5$, $\omega_{C'} = 3$ and $\bar{n} = 6$. The initial state of the system is: $|\alpha_0\rangle = |1 + 3i\rangle$.

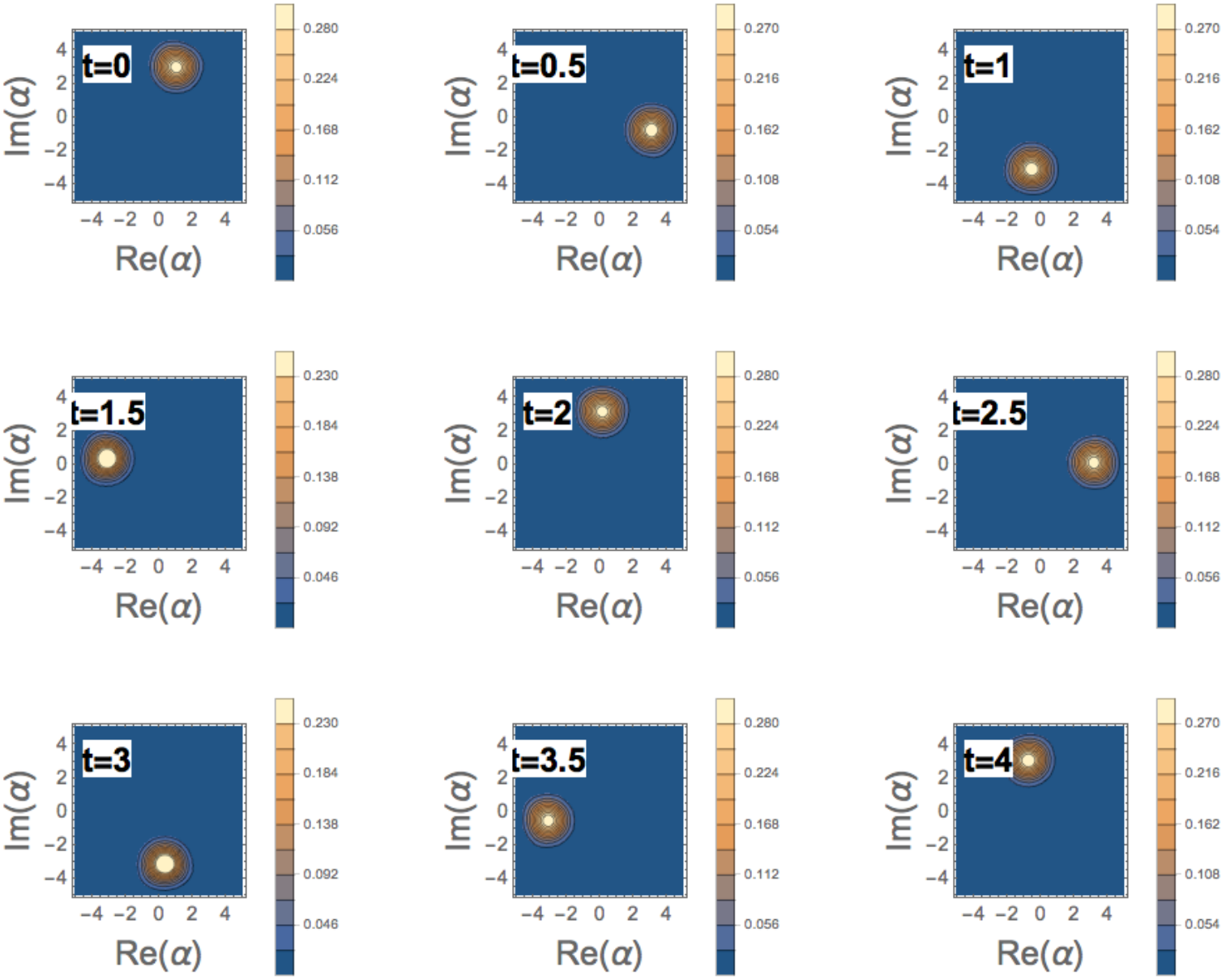

Figure 19: Husimi representation for a cavity mode driven by thermal light where the parameters used are: $\kappa = 0$ (there is no coupling), $\omega_{C'} = 3$ and $\bar{n} = 6$. The initial state of the system is: $|\alpha_0\rangle = |1 + 3i\rangle$.

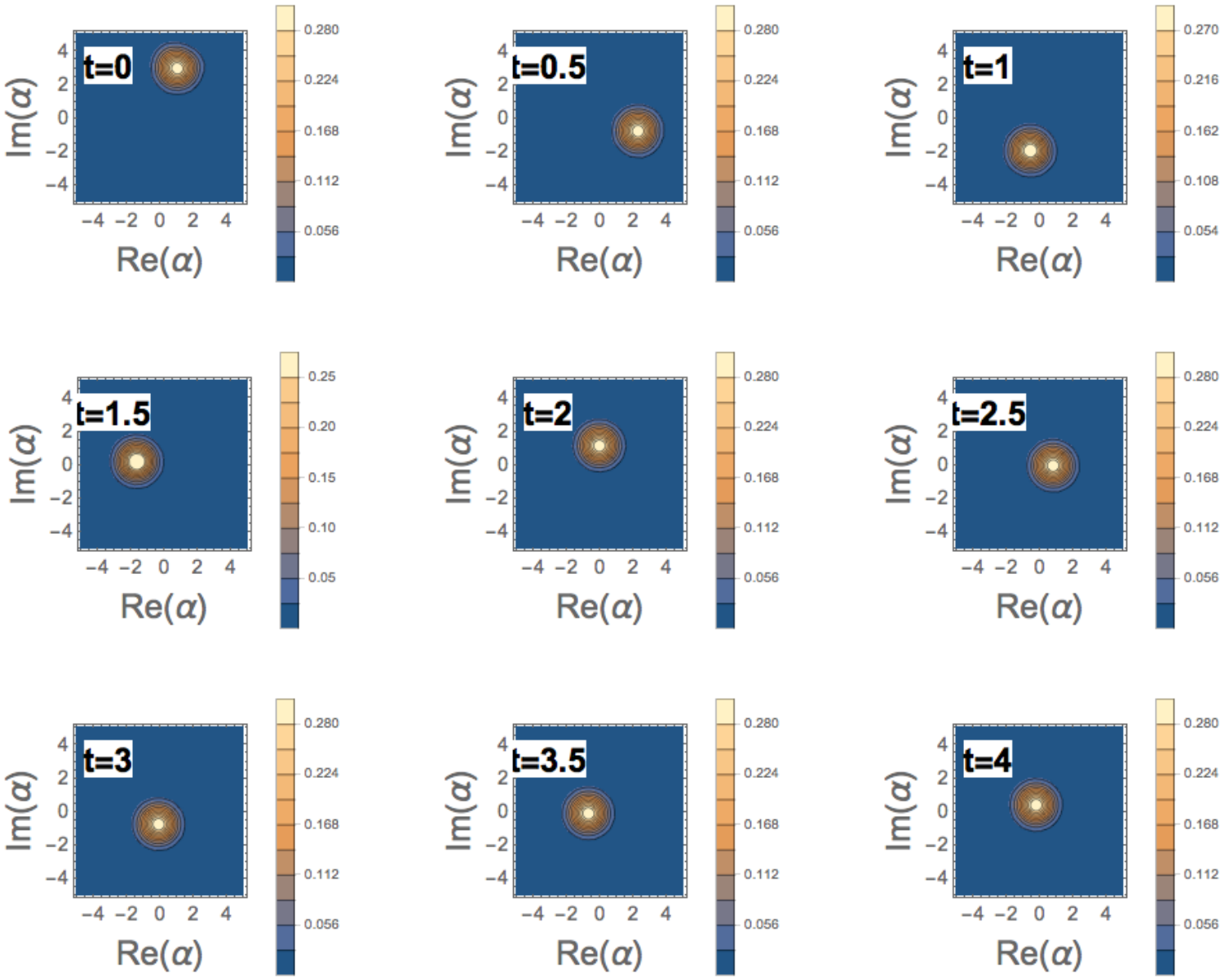

Figure 20: Husimi representation for a cavity mode driven by thermal light subjected to an electric field, where the parameters used are: $\kappa = 0.5$, $\omega_{C'} = 3$, $\eta = 0.5$ and the reservoir is in the vacuum state ($\bar{n} = 0$). The initial state of the system is: $|\alpha_0\rangle = |1 + 3i\rangle$.

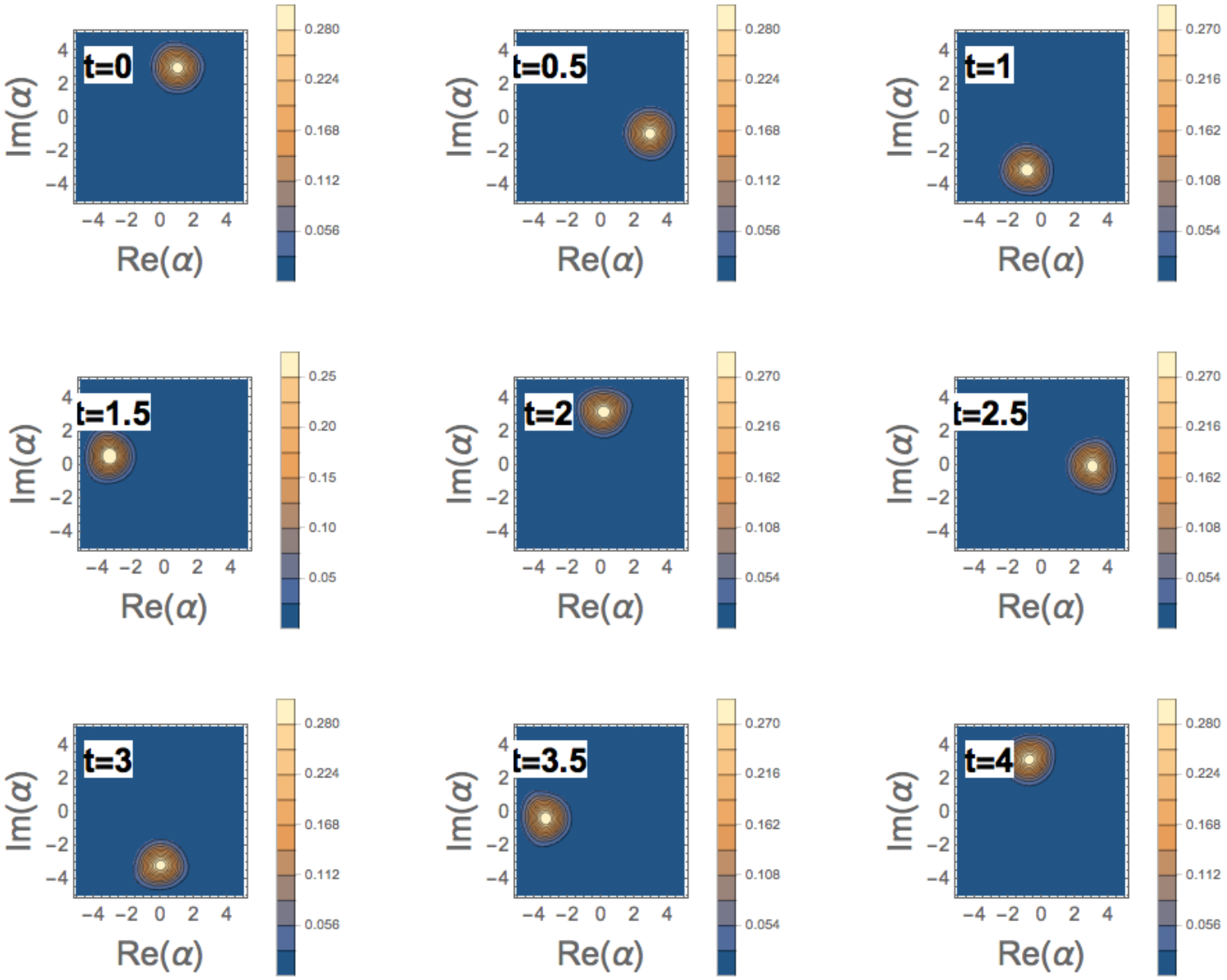

Figure 21: Husimi representation for a cavity mode driven by thermal light subjected to an electric field, where the parameters used are: $\kappa = 0$ (no coupling), $\omega_{C'} = 3$, $\eta = 0.5$ and the reservoir is in the vacuum state ($\bar{n} = 0$). The initial state of the system is: $|\alpha_0\rangle = |1 + 3i\rangle$.

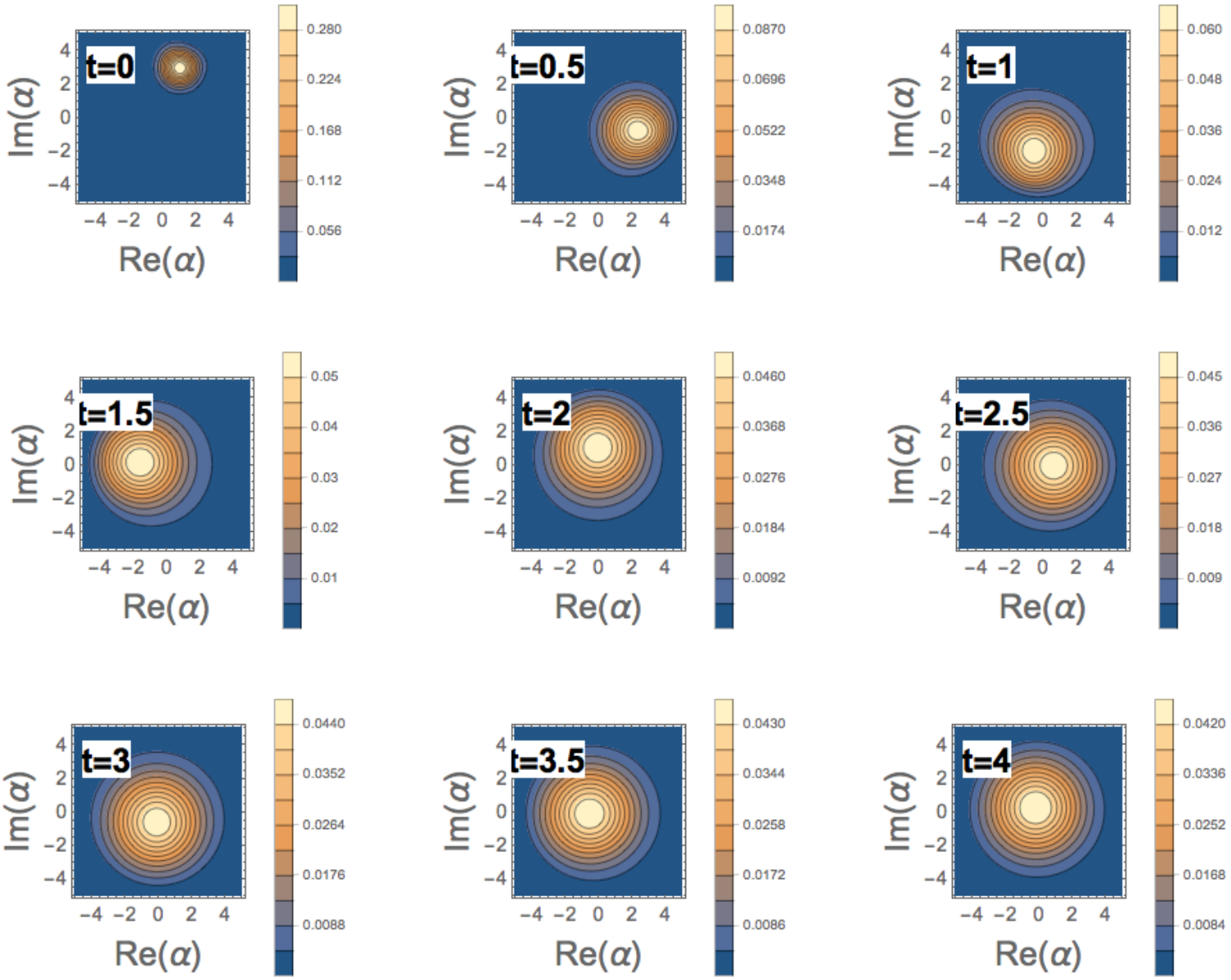

Figure 22: Husimi representation for a cavity mode driven by thermal light subjected to an electric field, where the parameters used are: $\kappa = 0.5$, $\omega_{C'} = 3$, $\eta = 0.5$ and $\bar{n} = 6$. The initial state of the system is: $|\alpha_0\rangle = |1 + 3i\rangle$.

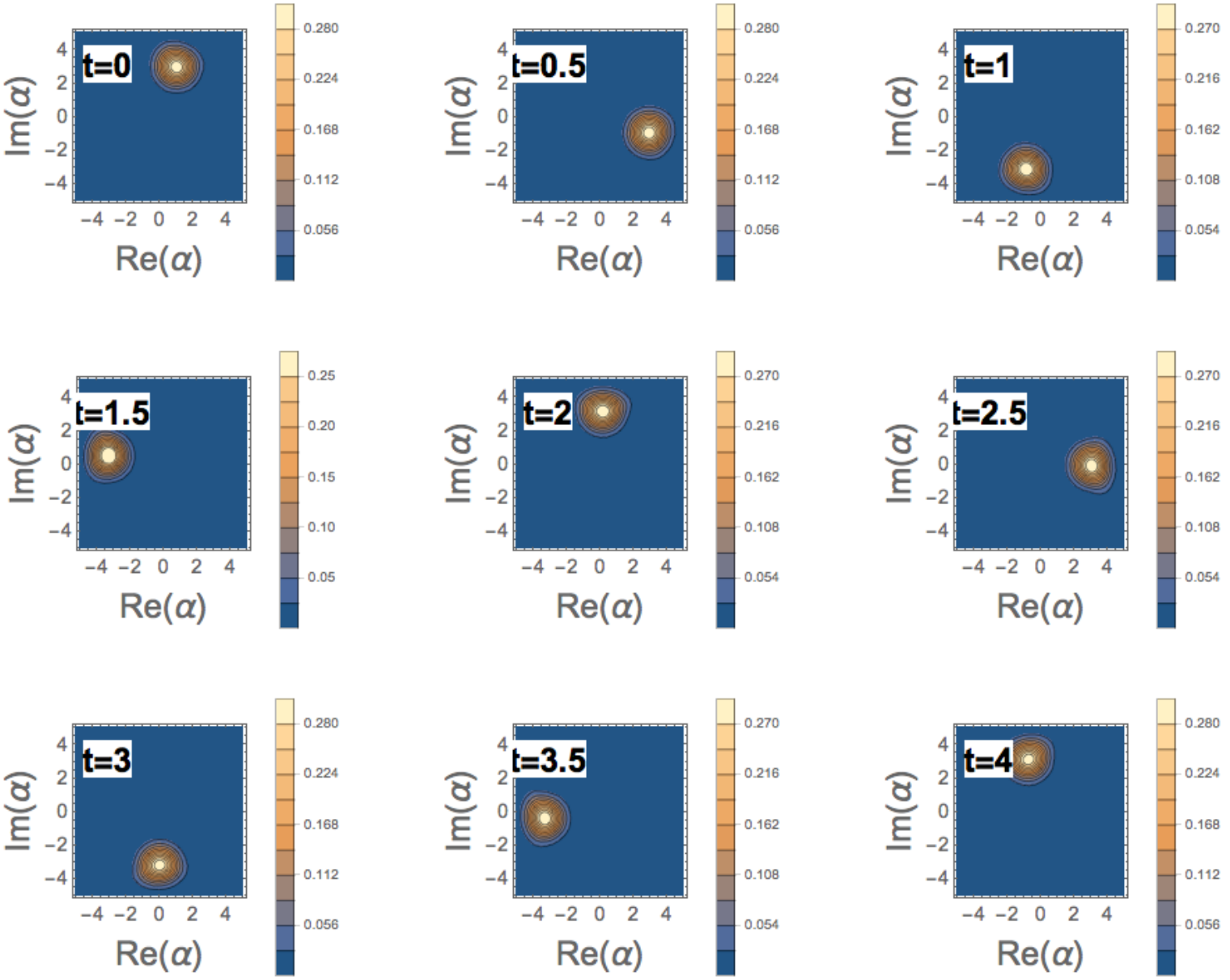

Figure 23: Husimi representation for a cavity mode driven by thermal light subjected to an electric field, where the parameters used are: $\kappa = 0$ (no coupling), $\omega_{C'} = 3$, $\eta = 0.5$ and $\bar{n} = 6$. The initial state of the system is: $|\alpha_0\rangle = |1 + 3i\rangle$.